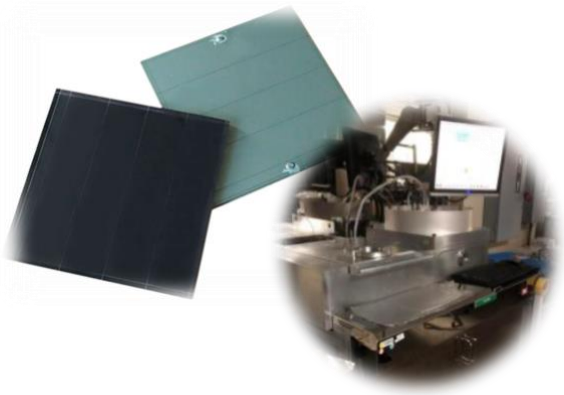

Photoconductivity Characterization and Evaluation of High Density Plasma Chemical Vapor Deposited (HDPCVD) Amorphous Silicon (a-Si:H) Films

ENGR 241 Final Report

Spring Quarter 2022

June 10, 2022

Mo Wu & Wei Ren

Instructor: Prof. Roger Howe

Mentors: Usha Raghuram, Swaroop Kommera, Lavendra Yadav Mandyam

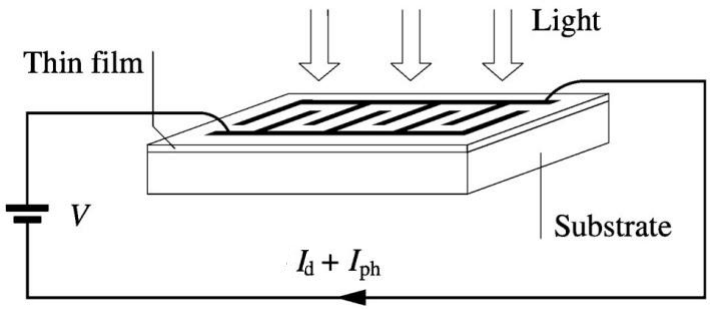

Table of Contents

1. Executive Summary

1.1. Summary of Work performed

The goal of this project is to find a recipe for high density plasma chemical vapor deposition (HDPCVD) that maximizes photoconductivity of hydrogenated amorphous silicon (a-Si:H) thin film without compromising the deposition qualities (such as the deposition rate, surface roughness, and uniformity). More than two dozen, one-hour depositions on silicon dioxide coated Si wafers were performed. An initial round of experiments were carried out as a screening test to determine the four main effects out of six independent controls of the deposition tool. The second-round experiments were a fine-tuning set to study the interaction effects between the two main effects. *Figure 1* shows a selection of significant depositions.

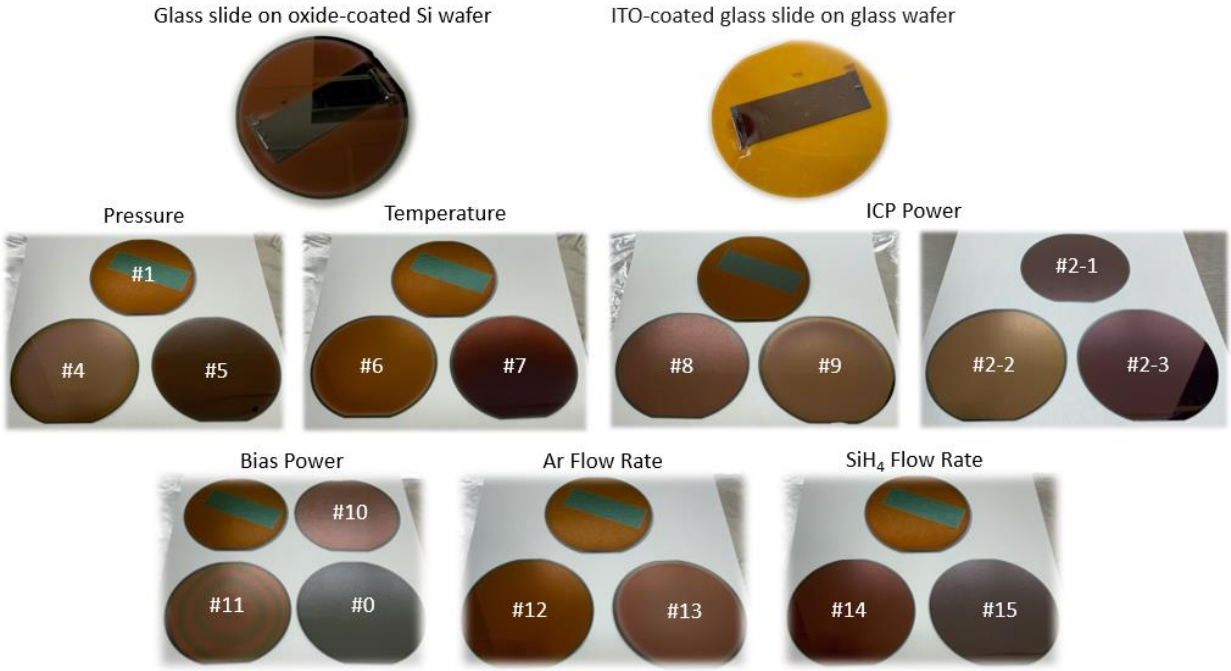

Figure 1 Selected a-Si:H depositions. The top two figures are testing samples used to determine the substrate. The following figures are samples varying different deposition parameters. The numbers refer different recipes which will be explained more in later chapters.

For the conductivity measurement, three different designs for electrical ohmic contact were tested and we ended up using an interdigitated electrode configuration with 150nm Au on top of a 40nm Ti adhesion layer. *Figure 2* shows the image of the patterned wafer after photolithography, metal deposition and lift-off, and our design of interdigitated electrodes (drawn using the GDS editing software CleWin).

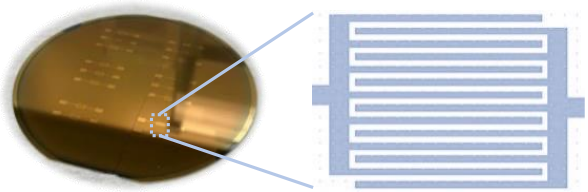

Figure 2 Interdigitated electrodes design. The left figure shows the a-Si:H deposited wafer with electrical contact pads. The right figure shows the design of the interdigitated electrodes.

The photoconductivity measurement setup, shown in Figure 3, was built in the Hesselink lab. We measured bright and dark currents to determine the photoconductivity as photosensitivity ratio ($\sigma_{light}/\sigma_{dark}$). All depositions were characterized for the photoconductive performance. *Figure 4* is an overview of the photoconductive response of HPDCVD a-Si:H thin films with respect to six deposition factors and time.

(a)

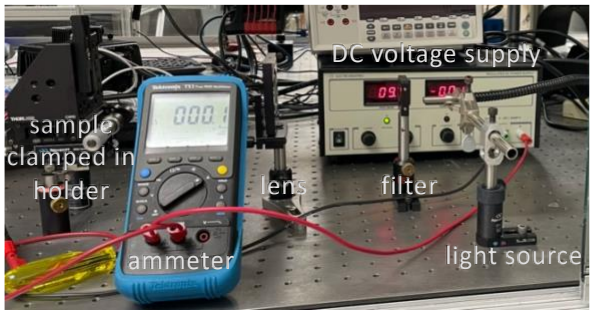

(b)

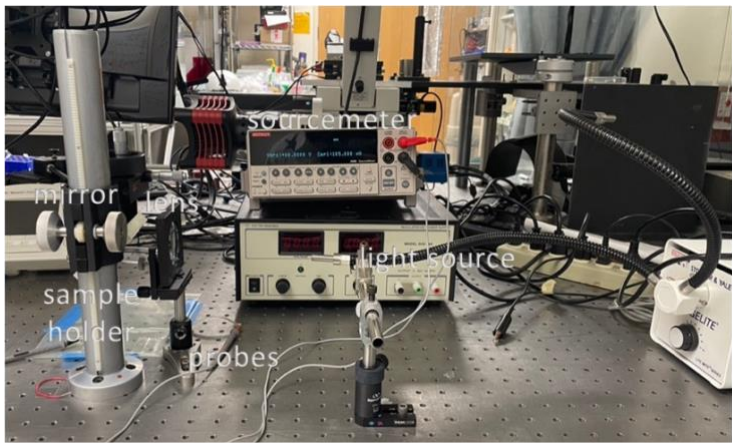

Figure 3 Photoconductivity measurement experimental setup. (a) The first-generation setup. (b) The second-generation setup where we replaced the DC voltage supply with a Keithley 2400 sourcemeter for performance concern.

An optimal recipe which gives the largest photoconductivity ratio was determined as shown in *Table 1.* Note that this recipe is optimal among the more-than-two-dozen, one-hour depositions we performed. Time effect for photoconductivity was also studied but no significant impact on the photoconductive performance was observed.

Table 1 Summary of the HDPCVD a-Si:H recipe for maximal photoconductivity

Optimal Photoconductivity Recipe	
Pressure	4mTorr
Temperature	90°C
ICP Power	1800W
Bias Power	0W
Ar Flow Rate	40sccm
SiH4 Flow Rate	4sccm

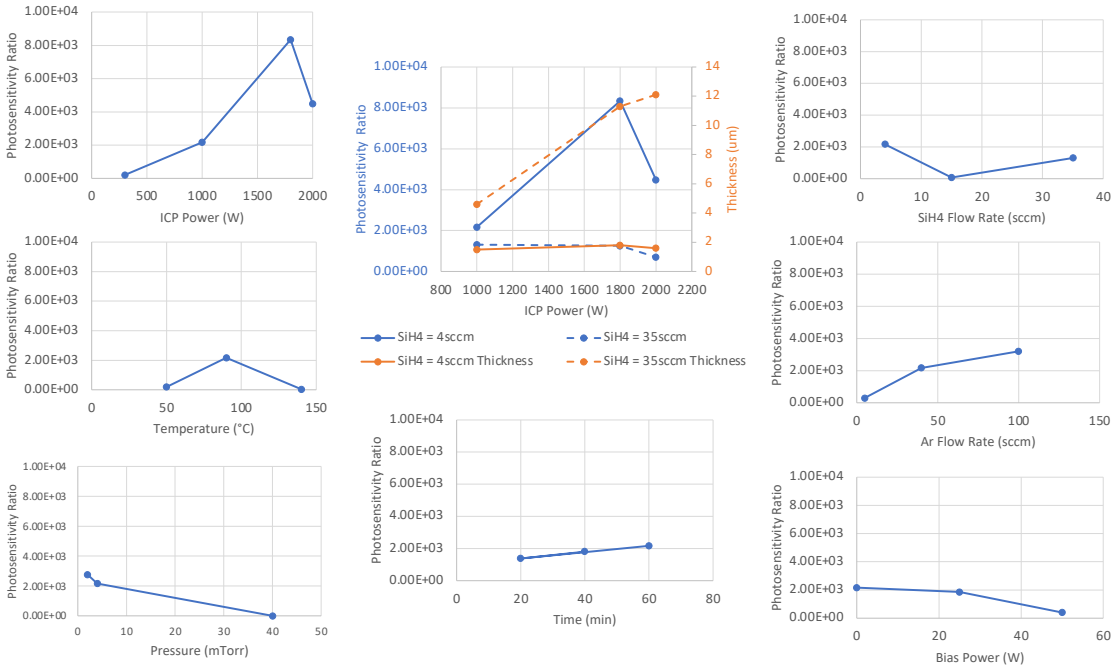

Figure 4 Photoconductivity measurement overview regarding different deposition parameters.

1.2. Benefits to the SNF Community

We believe that our work can be beneficial to the SNF community. We have identified three unique application cases where our work can be useful: Frist, we offer a guideline to build photoconductivity measurement setup for a-Si:H thin film. Up to the time we submit the report, there is no available shared equipment to measure photoconductivity of thin-films at SNF/SNSF. Our protocol could facilitate quick development of photoconductivity measurement setup to those who are interested. The experimental setup could also be used for other photoconductive thin films. The Hesselink lab is also willing to collaborate on relevant photoconductive material research.

Second, we explored the optimal HDPCVD recipe regarding photoconductivity and provide the first documentation on characterization of a-Si:H photoconductivity in the SNF community. Additional deposition qualities (e.g., deposition rate, thickness uniformity, surface roughness, refractive index, etc.) were also measured and summarized. These data are a good foundation for Stanford research groups interested in photoconductive films.

Last but not the least, two standard operating procedures (aka Nano Nuggets) were developed during the course of our project:

1. Photoconductivity measurement setup protocol
2. Post analysis for AFM raw images using Gwyddion

2. Introduction

2.1. Motivation

Amorphous silicon (a-Si:H), unlike crystalline materials, amorphous materials lack long range periodicity in their structure. This inherent characteristic actually makes it a fantastic photoconductive material due to its high efficiency to absorb light energy. Its efficiency to absorb solar radiation can be as high as an order of magnitude higher than that of the single-crystal silicon. It is a broadband radiation absorber in the sense that 90% of incident light would be absorbed by a film of around 1μm thick [1]. There are other economic advantages. For example, it could be deposited under a relative low temperature around 200-300 degree Celsius, which allows deposition on inexpensive substrates, such as metal, glass, and plastic [1]. All those characteristics enable a-Si:H to be compatible with mass production. Due to the great performance in both scientific and economic aspects, a:Si-H is used in a wide range of applications such as solar cells, photo-emissive devices (e.g. organic light-emitting diodes (OLEDs)), optoelectronic devices, display backplane transistors, and medical imaging[2].

Photoconductivity is a key physical parameter which quantifies the potential of a material to be used as an opto-electric converter. However, there are no relevant documentations on photoconductive performance characterization at SNF/SNSF since there are no suitable tools to measure it directly. Thus, we built an experimental setup in the Hesselink lab to measurement the photoconductivity of a-Si:H thin films. We searched for an optimal recipe on available CVD tools to maximize the photoconductivity with acceptable deposition qualities. Along with the photoconductive performance measurement, additional optical parameters and film quality data were collected to supplement the SNF database, such as deposition rate, thickness uniformity, surface roughness, and refractive index.

2.2. Previous Work

In the past half century, there have been numerous techniques developed to measure the a-Si:H thin film photoconductivity and other affiliated properties. To name a few, there are steady-state photoconductivity method (SSPC), constant photocurrent method (CPM), steady-state photocarrier grating method (SSPG), modulated photocurrent spectroscopy (MPC), and transient photocurrent spectroscopy (TPC). Some of them have been developed and improved by generations of researchers. For example, CPM was applied by Vaněček et al. [3] to study the deep defect density back in 1995 while the same method with advanced design was implemented to study the defect by Malik et al. in 2019 [4]. SSPG has also been addressed several times [5-7] on the photoconductive study of different types of a-Si:H. *Figure 5* is a flowchart of selected recent progress [3-8] on photoconductivity measurement.

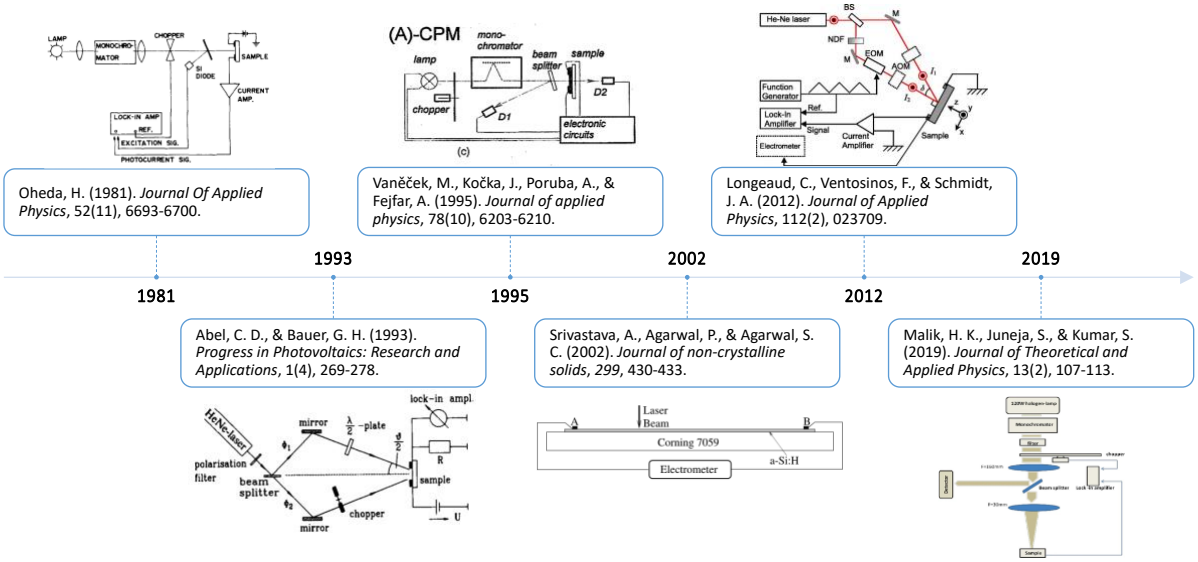

Figure 5 Flowchart of selected recent progress on photoconductivity measurement.

2.3. Project Outline

The goal of our project is summarized in *Figure 6*.

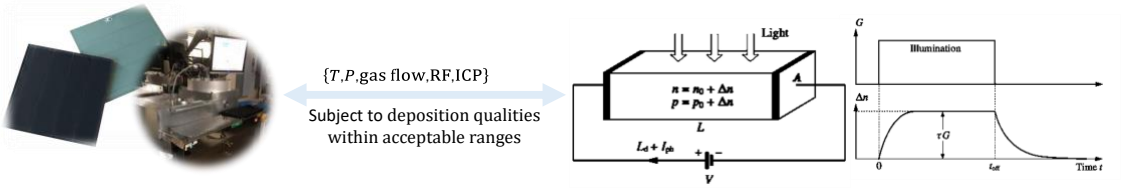

Figure 6 Graphic illustration of the project objective to maximize the photoconductivity of HDPCVD a-Si:H thin film [10].

We limited ourselves to HDPCVD as the deposition equipment because the plasma enhanced CVD (PECVD) tool has been down. In the following chapters, we will first explain our fabrication process flow and design of experiments (DOE), followed by our photoconductivity characterization experimental setup. Then we will show our results of film quality characterization and photoconductivity measurement. Analysis for each factor of each design is discussed. We will conclude with our major findings and outlook for future work.

3. Fabrication and Experiments

3.1. Process Flow

Figure 7 is an overview of our fabrication process flow. To start off, before the a-Si deposition, a 300nm silicon dioxide layer is deposited using the same tool (HDPCVD) to introduce an insulating layer as well as a buffer layer between Si wafer and deposited a-Si:H. Then we carry on the a-Si:H deposition based on our DOE. Afterwards, we collect the data of the film's optical properties using Woollam in order to calculate the film uniformity later. With the deposition finished, we pattern our wafer with photolithography and deposit metal contact pads through lift-off. After lift-off, we are done with all the cleanroom process so that we can cleave the wafer to characterize its thickness/deposition rate (using SEM) and surface roughness (using AFM). With a confident estimate of film thickness, uniformity can then be calculated based on the data previously collected from Woollam. The final step is to measure the photoconductivity with the setup built in the Hesselink lab. Now we will dive into each step in detail.

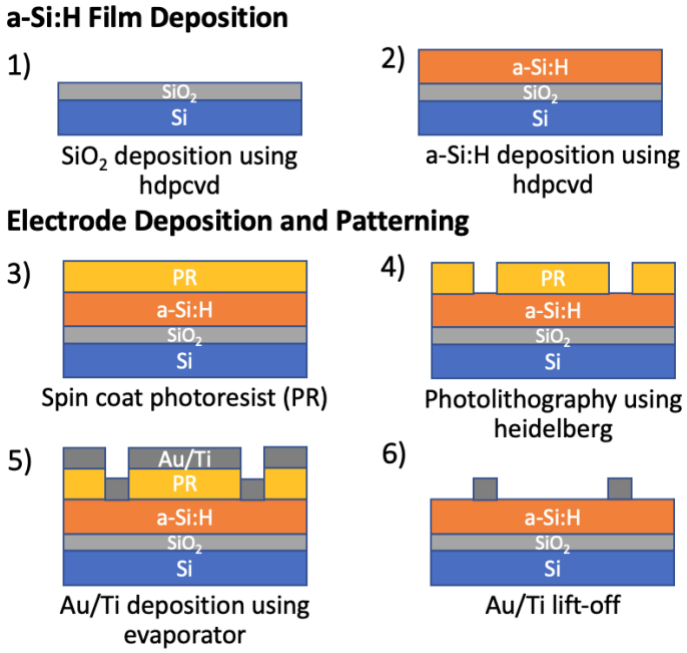

Figure 7 Process flow overview. The process includes two main components, a-Si:H film deposition and electrode deposition and patterning.

3.1.1. HDPCVD a-Si:H Deposition

Configuration

Regarding any deposition, there are three things we considered: which tool to use, what substrate to deposit on, and how long to deposit for.

For the tool selection, both PlasmaTherm Shuttlelock PECVD System (ccp-dep) and PlasmaTherm Versaline HDP CVD System (HDPCVD) at SNF were considered. Higher temperature and higher pressure are usually preferred for higher quality film deposition, while lower deposition temperature and pressure could be compensated by higher involvement of plasma. For a-Si:H, low temperature is preferred to maintain its amorphous structure instead of being crystallized. Since the ccp-dep has been down for a long period throughout the quarter, we decided to focus on HDPCVD for our purpose.

Regarding the substrate, we test on four different types: ITO-coated glass slide, glass slide, SiO_2 coated Si wafer, and glass wafer as shown in *Figure 8*. We first tried a top-down electrode configuration using ITO-

coated glass slide as shown in the left part of *Figure 9*. The motivation was to avoid electrode deposition. However, we found that the contacts were not ohmic, which we will discuss later, so we shifted to wafer substrates. Both glass wafer and SiO_2 coated Si wafer would work for us with standard patterned electrodes for the photoconductivity measurement. Glass wafer is actually better in the sense that it would allow backside illumination. However, due to the supply shortage of glass wafer, we ended up with silicon dioxide coated Si wafer as shown in the right of *Figure* 9.

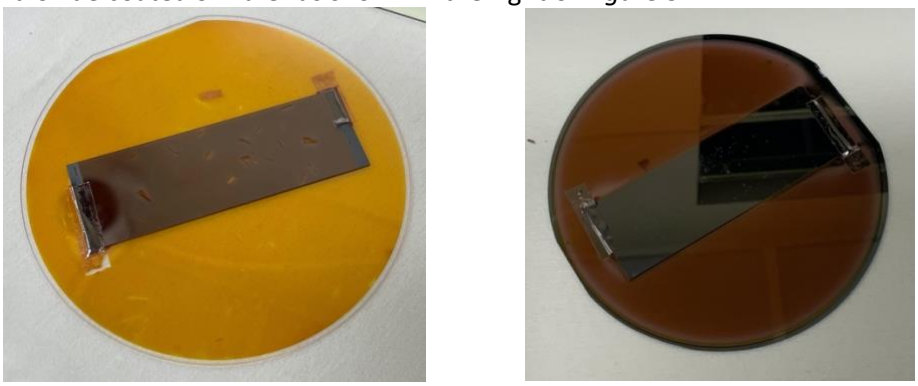

Figure 8 a-Si:H deposition on 4 different substrates (standard recipe for 60min). Left figure includes an ITO-coated glass slide on top of a glass wafer. Right figure includes a glass slide on top of a Si wafer.

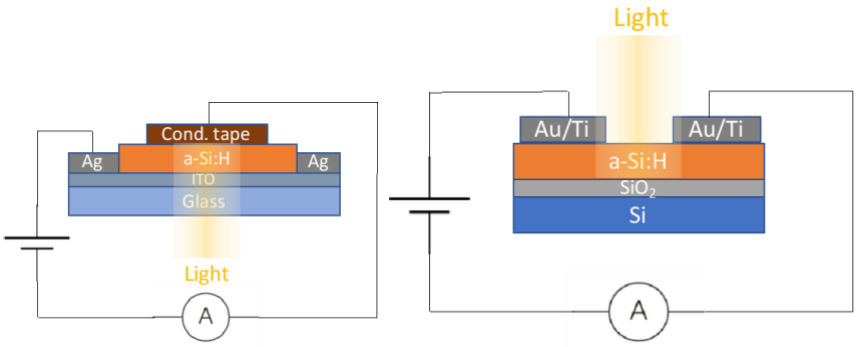

Figure 9 Schematic of the photoconductivity measurement setup for samples on ITO-coated glass slide substrate (left) and on SiO_2 coated Si wafer substrate (right).

Finally for the deposition time, we adopted the recipe from some literatures [9,14,15] where researchers used 1μm thick a-Si:H as a standard. For the standard HDPCVD recipe provided by SNF staff, it takes an hour to obtain around 1μm thickness. Thus, we kept the deposition time as 60min. Few of our samples were deposited for shorter period of time to study the deposition time effect, but for the majority of them it was one hour for the control purpose.

Intermediate SiO_2 Layer Deposition

Before any depositions, it is good to clean away hydrocarbons on the surface immediately before the deposition. We carried out the following pre-cleaning procedure:

- Step 1: Acetone/Methanol/Isopropanol rinse and N_2 dry.
- Step 2: O_2 plasma clean (technics, O_2, ~300mTorr, 50W, 1min)

For the SiO_2 deposition, we used HDP_SiO2 recipe. The deposition rate was around 150-160nm/min. We ran it for 2min to obtain 300nm SiO_2 layer. A 2min seasoning was run before the deposition. *Figure 10* shows the first and last depositions among a batch of nine samples. We used Woollam to characterize the intermediate layer thickness for both two wafers and same thickness values were obtained for around 300nm. More detail is included in the Appendix.

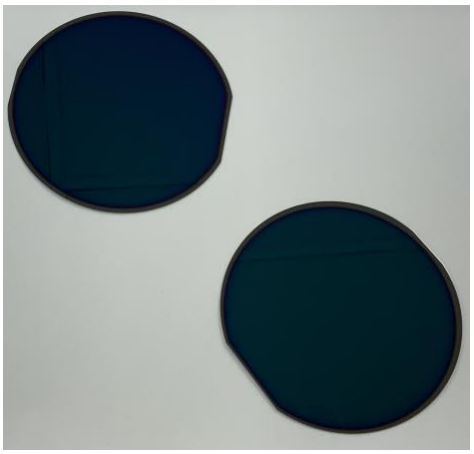

Figure 10 SiO_2 deposited on Si substrate. The top one is the first deposition while the bottom one is the last deposition among a batch of nine silicon dioxide coated Si wafers.

a-Si:H Deposition

For a-Si:H deposition, we adopted Lavendra_HDP_a-Si recipe into our own WR_HDP_a-Si recipe to figure out the recipe giving the best photoconductivity based on our own DOE. DOE will be discussed more in the next sub-chapter. Now we just show all the relevant depositions in *Figure 11-17*.

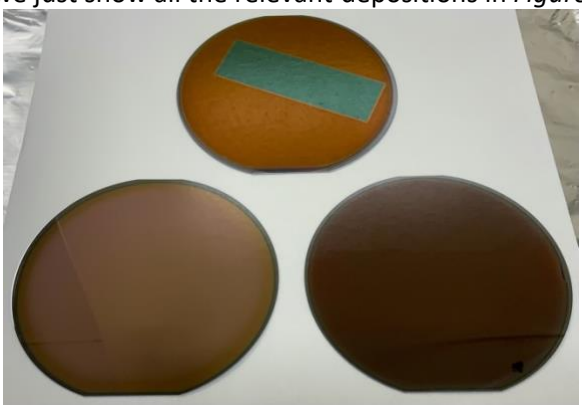

Figure 11 a-Si:H depositions with different pressure.
Top (standard recipe): P=4mTorr. Bottom left: P=2mTorr. Bottom right: P=40mTorr.

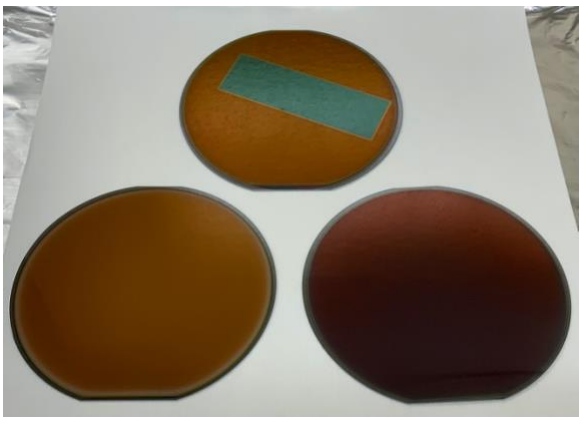

Figure 12 a-Si:H depositions with different temperature.
Top (standard recipe): T=90˚C.
Bottom left: T=50˚C. Bottom right: T=140˚C.

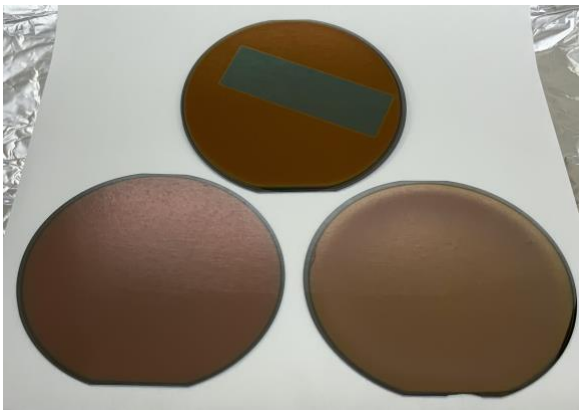

Figure 13 a-Si:H depositions with different inductively coupled plasma (ICP) power.
Top (standard recipe): ICP=1000W.
Bottom left: ICP=300W. Bottom right: ICP=1800W.

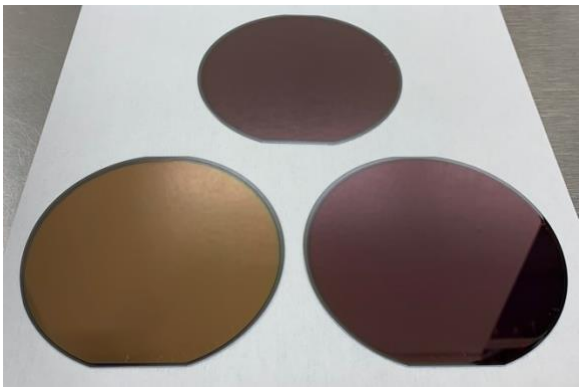

Figure 14 a-Si:H depositions with different ICP power and SiH_4 flow rate.
Top: ICP=1800W, SiH_4=35sccm.
Bottom left: ICP=2000W, SiH_4=4sccm. Bottom right: ICP=2000W, SiH_4=35sccm.

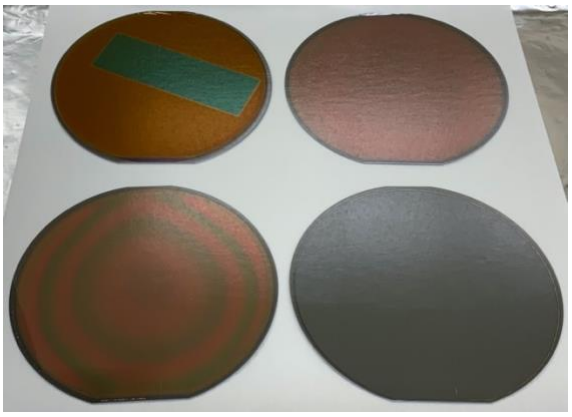

Figure 15 a-Si:H depositions with different bias power (BP).
Top left (standard recipe): BP=0W. Top right: BP=25W.
Bottom left: BP=50W. Bottom right: BP=100W (Totally etched).

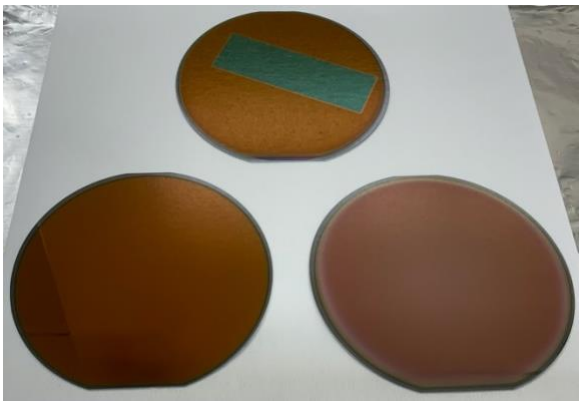

Figure 16 a-Si:H depositions with different Ar flow rate
Top: Ar=40sccm.
Bottom left: Ar=5sccm. Bottom right: Ar=100sccm.

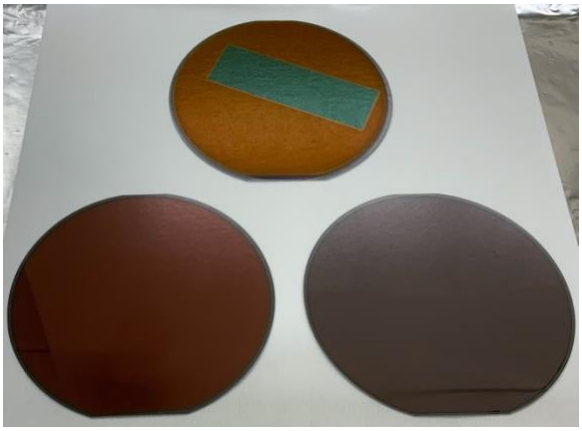

Figure 17 a-Si:H depositions with different SiH_4 flow rate
Top: SiH_4=4sccm.
Bottom left: SiH_4=15sccm. Bottom right: SiH_4=35sccm.

3.1.2. Electrode Deposition and Patterning

Electrodes were defined by lithography. 1.6μm SPR3612 was spin coated by svgcoat2 with vapor prime and 2mm EBR. Then the sample was exposed by Heidelberg with a dose of 100 mJ/cm^2 and a defocus of -2. (For the sample with glass substrate the dose was increased to 130 mJ/cm^2. However, some almond shaped speckles appeared after lift-off. An underexposure was suspected after analysis.)

The metal material for the contact pads was chosen so that it can make good ohmic contact with the a-Si:H film surface. We first tried to use 150nm aluminum deposited by Leybold Univex Sputter (*Figure 18*). Then we tried to evaporate 40nm Ti and 150nm Au (*Figure 19*), because according to [11], Ti makes better ohmic contact with a-Si:H than Al. To make better electrical contact, a 1min HF (50:1 concentration) bath was performed to etch away the native Si oxide accumulated after a-Si deposition. Ohmic contact was observed in the majority of our samples.

The metal layer lift-off was accomplished by an overnight (more than 24 hours) acetone bath. The loosened metal layer was sprayed off with acetone using a squeeze bottle. An ultrasonic bath was used for 2min maximum to get rid of the stubborn metal pieces. Then the sample was sprayed with acetone followed by isopropanol using a squeeze bottle. Finally, the sample was blow dried with N_2 gun.

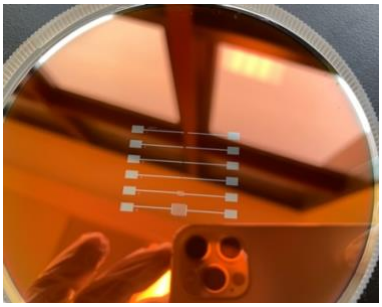

Figure 18. Al/a-Si:H/SiO2/Si sample. a-Si:H was deposited by the standard recipe for 60min.

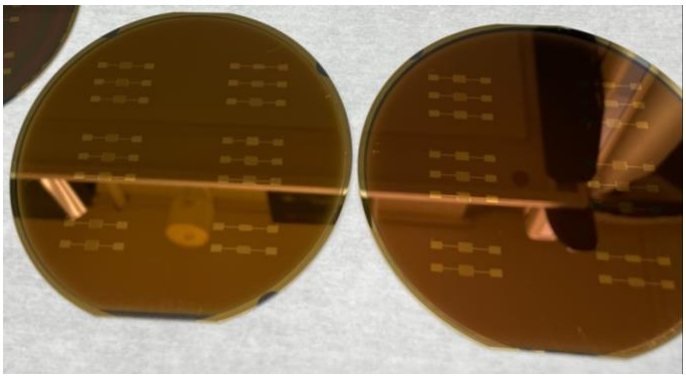

Figure 19. Au/Ti/a-Si:H/SiO2/Si samples. a-Si:H was deposited by the standard recipe for 40min (left) and 60min (right).

3.2. Design of Experiment (DOE)

3.2.1. Screening for Main Effects

Table 2 is a summarization of our DOE for the parameter screening purpose. Unlike standard DOE that starts from scratch, we already have a good reference (#1) recipe provided by Dr. Lavendra Mandyam, SNF process engineer. This fact makes DOE algorithms like JMP unnecessary. If we used JMP, it would be a model with multiple 3-level factors which would double the experiments we design. Considering about the budget and time, we studied on each variable independently, varying the factor to its upper and lower limits.

Table 2 First round of DOE for parameter screening test.

Recipe Name	Time (mins)	Pressure (mTorr)	Temperature (°C)	ICP Power (W)	Bias Power (W)	Ar Flow Rate (sccm)	SiH_4 Flow Rate (sccm)
#1	60	4	90	1000	0	40	4
#2	20	4	90	1000	0	40	4
#3	40	4	90	1000	0	40	4
#4	60	2	90	1000	0	40	4
#5	60	40	90	1000	0	40	4
#6	60	4	50	1000	0	40	4
#7	60	4	140	1000	0	40	4
#8	60	4	90	300	0	40	4
#9	60	4	90	1800	0	40	4
#10	60	4	90	1000	25	40	4
#11	60	4	90	1000	50	40	4
#0 (Etch out)	60	4	90	1000	100	40	4
#12	60	4	90	1000	0	5	4
#13	60	4	90	1000	0	100	4
#14	60	4	90	1000	0	40	15
#15	60	4	90	1000	0	40	35

3.2.2. Interaction Effects

After the screening test, we focused on two selected main factors: ICP power and SiH_4 flow rate, and studied further for their correlation. The photoconductivity increased linearly with the ICP power and followed a convex quadratic relationship for SiH_4 flow rate. We wanted to see 1) whether there is any boosting performance if we keep increasing ICP power and 2) for a fixed ICP power, whether one SiH_4 flow rate is better than the other for the two boundary values. We will discuss them more later. The other two main factors are temperature and Ar flow rate. Those would be studied in the future.

Table 3 2nd round of DOE for interaction effect study between ICP power and SiH_4 flow rate.

Recipe Name	Time (mins)	Pressure (mTorr)	Temperature (°C)	ICP Power (W)	Bias Power (W)	Ar Flow Rate (sccm)	SiH_4 Flow Rate (sccm)
#9	60	4	90	1800	0	40	4
#2-1	60	4	90	1800	0	40	35
#2-2	60	4	90	2000	0	40	4
#2-3	60	4	90	2000	0	40	35

3.3. Photoconductivity Measurement Protocol

To quantify the photoconductivity, photosensitivity ratio ($\sigma_{light}/\sigma_{dark}$) was chosen to be the measurable quantity. As conductivity is $\sigma = \frac{l}{RA}$, the photosensitivity ratio is simply the light and dark

current ratio $\frac{\sigma_{light}}{\sigma_{dark}} = \frac{l}{R_{light}A}\frac{R_{dark}A}{l} = \frac{I_{light}}{V}\frac{V}{I_{dark}} = \frac{I_{light}}{I_{dark}}$, where l and A are the geometrical parameters of the tested a-Si:H film sample. *Figure 20* includes a schematic and a photo of the photoconductivity measurement setup. A sourcemeter (Keithley 2400) was used to apply a DC voltage V and measure the current I across the tested sample. For each sample, the current measurement is taken at multiple voltage values. To measure the photoconductivity of thin films, coplanar electrodes are usually evaporated onto the film surface as contacts. The contacts need to be ohmic [10]. According to [11], Sc, Mg, and Ti form exceptionally good ohmic contacts with a-Si:H. Because Ti is a most commonly used material at SNF, Ti was chosen as the electrode material. For each sample, interdigitated electrodes were patterned by lithography. 40nm Ti (adhesion layer) was then evaporated on the a-Si:H film surface followed by 150nm of Au for better electrical conductivity. Interdigitated electrodes were used to increase the current reading so that a more reliable measurement could be obtained. *Figure 21* shows the interdigitated electrode pattern which consists of 32 pairs of 20μm wide electrodes with spacings of 20μm. To measure the light current I_{light}, the sample was illuminated by a broadband white light source with a measured intensity of 96mW/cm^2, which is close to the standard in photoconductivity characterization in the solar industry. The spectrum of the light source is shown in *Figure A1*.

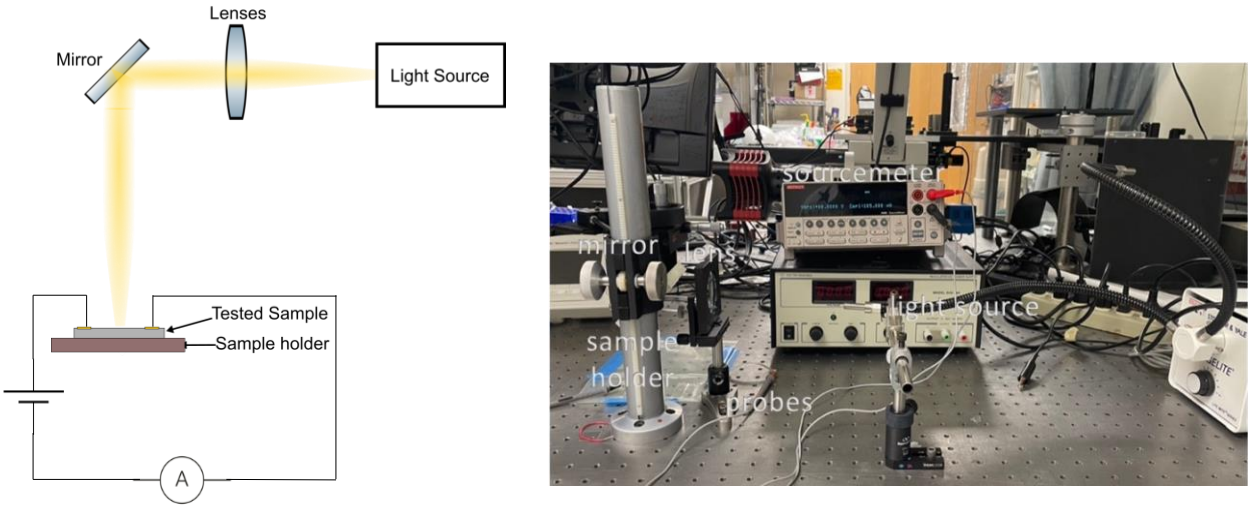

Figure 20 Schematic (left) and photo (right) of the photoconductivity measurement setup

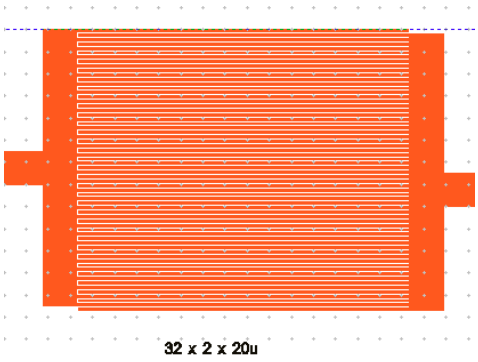

Figure 21 Interdigitated electrode pattern created with CleWin

4. Results and Discussions

4.1. Film Characterization

4.1.1. Deposition Rate

The film thickness of selected samples was measured by SEM. The sample was cleaved, and the cross section was imaged with a 2° tilt to avoid the electron accumulation caused by the insulating SiO_2 layer. The thicknesses of the film deposited with the standard recipe for 20, 40, and 60min are approximately 0.5, 1.0, 1.5μm (*Figure 22*), suggesting that the deposition rate of the same recipe is constant throughout the time, which is 250 Å/min. The ICP=2000W, SiH4=35sccm sample has a thickness of approximately 12μm (*Figure 23*). Such recipe has a deposition rate of 2000 Å/min, which is twice as much as the maximum value in the range given by [12]. The extremely high deposition rate may indicate a different reaction regime that creates polysilicon (poly-Si) instead of a-Si. On the other side, the cross section of this sample also seems much bumpier with more ridges, which might indicate more microvoids in the film.

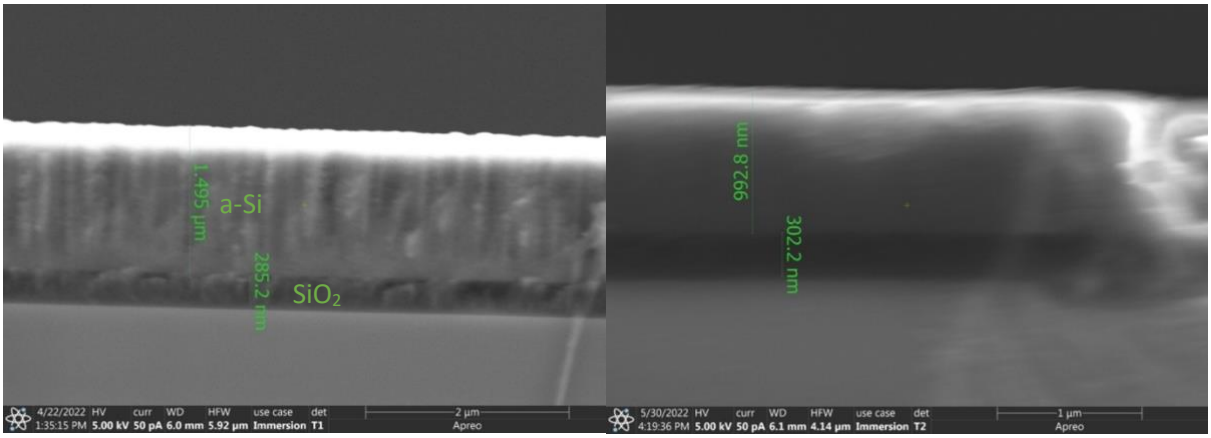

Figure 22 Cross section SEM image of the 60min (left) and 40min (right) samples

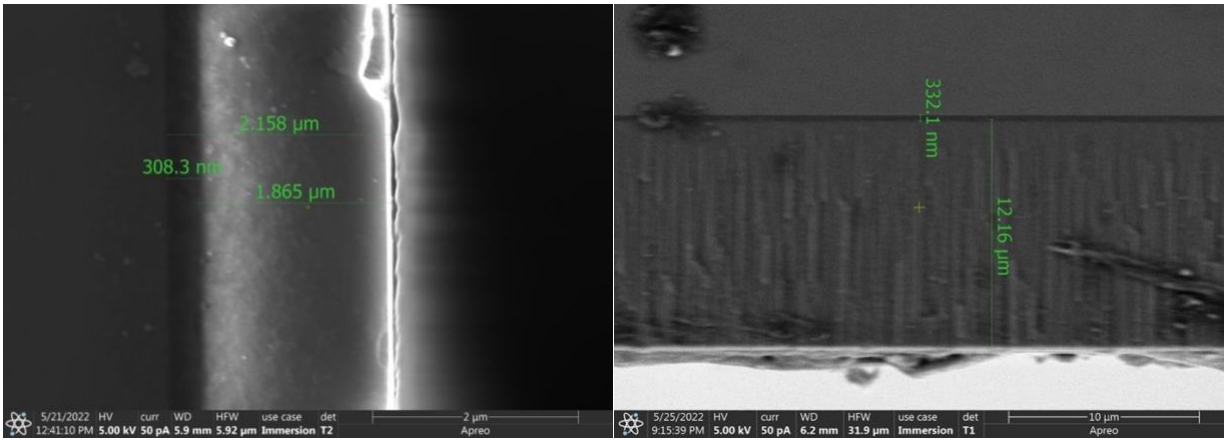

Figure 23 Cross section SEM image of the ICP=1800W, SiH_4=4sccm sample (left) and the ICP=2000W, SiH_4=35sccm sample (right)

We also tried the Woollam to measure the thin film thickness more economically; however, there seem to be multiple local optima which heavily depend on the initial thickness values. For example, for the #1 standard recipe, 1μm and 1.4μm initial thicknesses would both give good Woollam fittings. More details

are provided in *Figure A6*. Considering about this issue, we decided to use SEM cross-section imaging for the film thickness measurement and Woollam for verification purpose. After we obtained an accurate thickness, we could use collected data from Woollam ellipsometry to model and calculate the film uniformity.

4.1.2. Film Uniformity & Refractive Index

We used Woollam to calculate the film uniformity based on the thickness measurement from SEM. Right after the a-Si:H deposition, we carried out 5-point measurement on the wafer to collect ellipsometry data as shown in *Figure 24*. Once the electrodes were patterned, we cleaved the wafer to measure the film thickness. Then a more accurate thickness initial value could be input in WVASE software to model and fit for thickness values at the previous five points. With all five Woollam-measured thickness values, the uniformity could be calculated with the formula: $\text{Uniformity} = \frac{t_{\max} - t_{\min}}{2 \times t_{\text{avg}}} \times 100\%$, where $t_{\max}$, $t_{\min}$, t_{avg} are the maximum, minimum, average thickness of the 5 measured points.

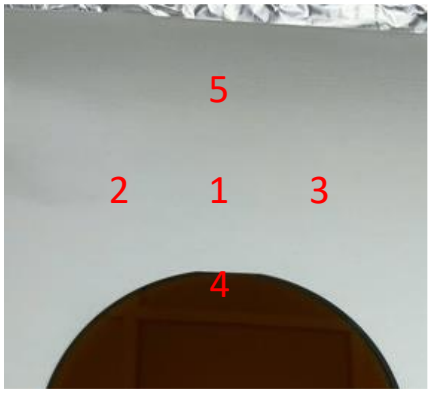

Figure 24 5-point measurement on a wafer to characterize film uniformity

One thing to notice is that although we inserted an initial thickness value measured from SEM, some ellipsometry data were hard to obtain a good fitting. Several cases resulted from the noisy data collected by Woollam, while some might have resulted from the deviation of deposited intermediate layer from default ideal SiO_2 whose refractive index data Woollam used to do the fitting. For further study on the film uniformity, refractive index of intermediate layer should be collected and used for subsequent fitting, which might lead to better thickness fitting. Uniformity of selected films are shown in *Table 4*. It represents an excellent uniformity less than 2%, which matches with the experience of other superusers for HDPCVD.

Table 4 Uniformity measurements of selected a-Si:H samples deposited by the corresponding recipes

Recipe Name	Time (mins)	Pressure (mTorr)	Temperature (°C)	ICP Power (W)	Bias Power (W)	Ar Flow Rate (sccm)	SiH4 Flow Rate (sccm)	Uniformity (%)
#1	60	4	90	1000	0	40	4	1.99
#9	60	4	90	1800	0	40	4	0.98
#2-1	60	4	90	1800	0	40	35	0.14
#2-2	60	4	90	2000	0	40	4	0.27

Refractive indices of the a-Si:H and SiO_2 layers in each sample were collected simultaneously when the Woollam ellipsometry measured the amplitude and phase information. Some of the raw data are summarized in the Appendix. The rest of the raw data are available upon request. Anyone interested

could use them for further study. *Figure 25* is an example of the ellipsometry data for #1 standard recipe as well as the good fitting generated by Woollam.

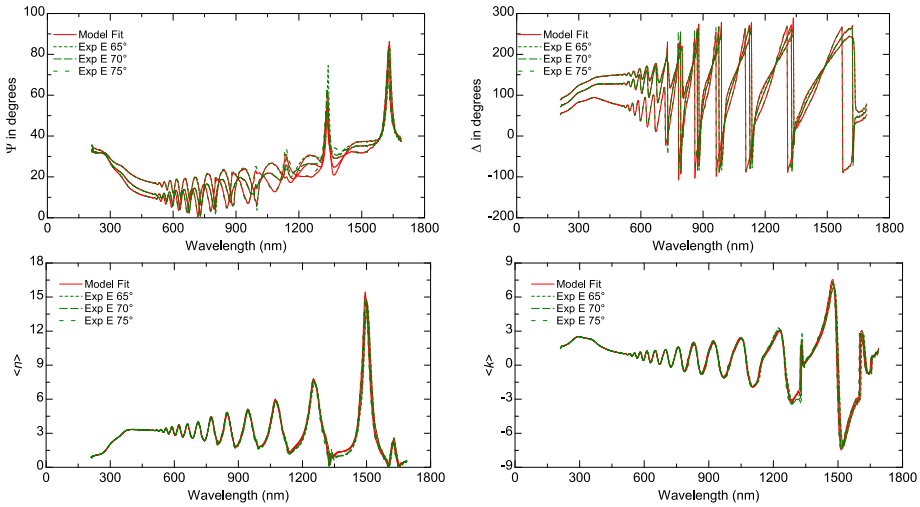

Figure 25 Woollam fitting for ellipsometry data of #1 recipe sample

4.1.3. Film Surface Roughness

We used SPM: Park XE-70 to measure the surface roughness of our depositions. Surface roughness is characterized by two quantities, root mean square height ($Sq = \sqrt{\frac{1}{A}\int\int_A Z(x,y)^2 dxdy}$) and arithmetical mean height ($Sa = \frac{1}{A}\int\int_A |Z(x,y)| dxdy$), where Z is the height and A is the are. Two sets of measurements were done: one for the surface roughness characterization regarding different substrates, and the other focusing on selected recipes after the photoconductivity measurement.

Figure 26 shows the AFM images for #1 recipe on four different substrates and *Table 5* is a summary of its surface roughness data. All images were processed with Gwyddion and a corresponding SOP was formulized to discuss about the post analysis procedure. We could see that all four substrates deposited using the same recipe have great surface quality considering the fact that the deposition thickness is around 1.5μm. Roughness values of SiO_2 coated Si wafer is slightly higher than other substrates, but the variance is totally acceptable especially taking the contribution of the intermediate SiO_2 layer into account.

Table 5 Surface roughness measurements of #1 recipe on four different substrates

Substrate	Surface Roughness Sq (nm)	Surface Roughness Sa (nm)
Oxide-coated Si wafer	21.90	17.92
ITO-coated glass slide	5.04	3.95
Glass slide	3.88	2.99
Glass wafer	3.77	2.73

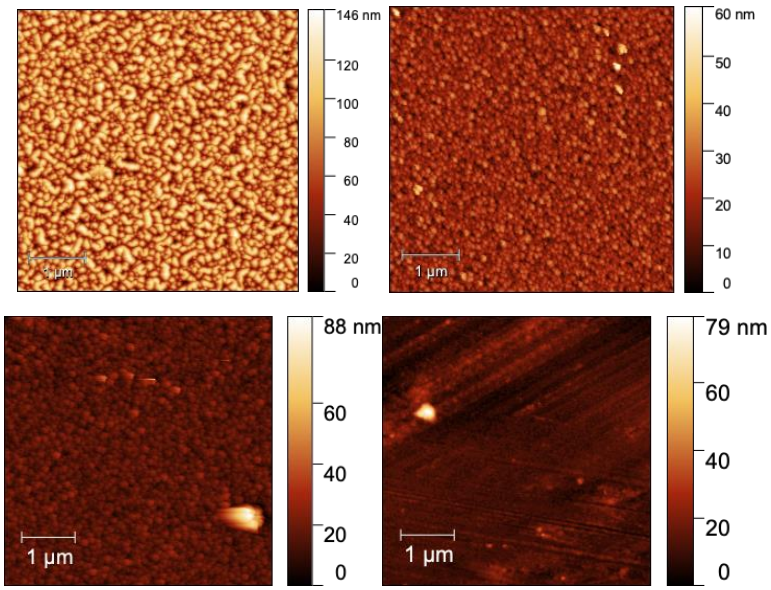

Figure 26 AFM images for #1 recipe on 4 different substrates.
Top left: SiO_2 coated Si wafer. Top right: ITO-coated glass slide. Bottom left: Glass slide. Bottom right: Glass wafer.

Figure 27-29 show the AFM images of selected recipes which focus on the correlation study between ICP power and SiH_4 flow rate. *Table 6* summarizes the corresponding surface roughness data.

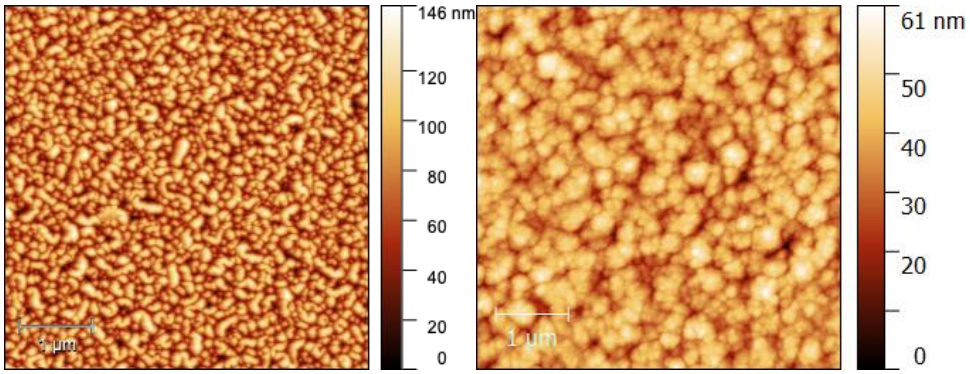

Figure 27 AFM images for #1 (left) and #15 (right) recipes

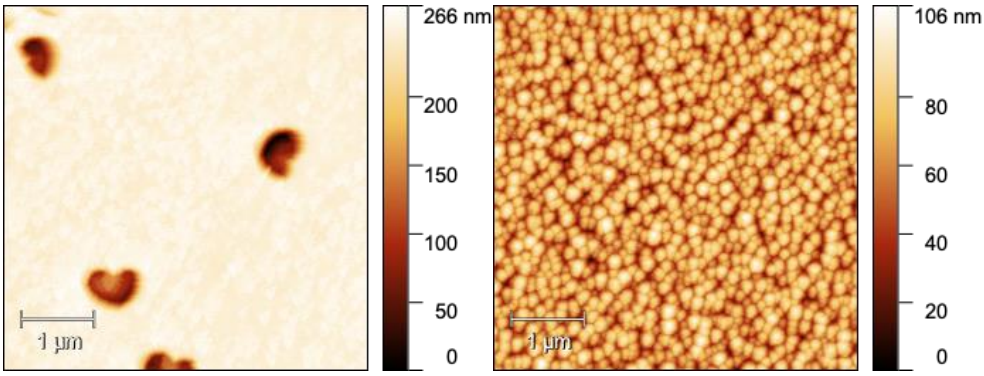

Figure 28 AFM images for #9 (left) and #2-1 (right) recipes

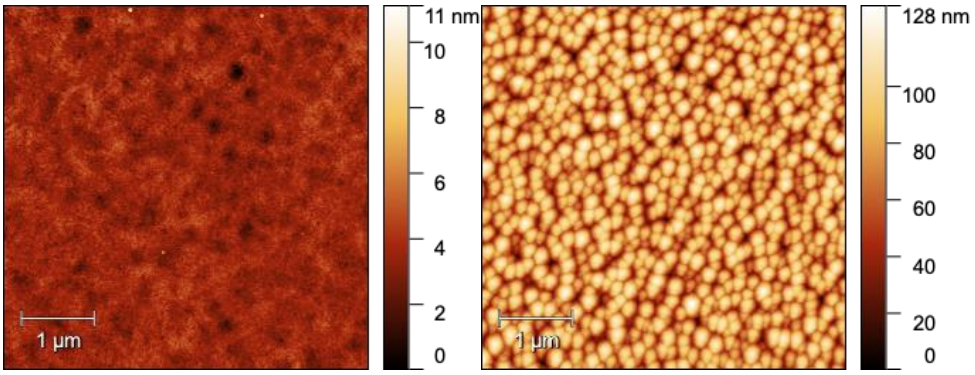

Figure 29 AFM images for #2-2 (left) and #2-3 (right) recipes

Table 6 Surface roughness measurements of the samples focusing on correlation study between ICP power and SiH_4 flow rate

Recipe Name	Time (mins)	ICP Power (W)	SiH_4 Flow Rate(sccm)	Surface Roughness Sq (nm)	Surface Roughness Sa (nm)
#1	60	1000	4	21.90	17.92
#15	60	1000	35	7.28	5.81
#9	60	1800	4	6.72	4.577
#2-1	60	1800	35	14.53	11.75
#2-2	60	2000	4	0.58	0.45
#2-3	60	2000	35	19.83	16.17

Clearly, there are interaction effects between ICP power and SiH_4 flow rate on the surface roughness. When SiH_4 flow rate is 4sccm, the surface roughness decreases as the ICP power increases; while it shows an opposite trend when SiH_4 flow rate is 35sccm.

4.2. Photoconductivity

The high-density plasma chemical vapor deposition (HDPCVD) has six independent parameters, pressure, temperature, inductively coupled plasma (ICP) power, bias power, argon flow rate, and silane flow rate. We screened each of these parameters and deposition time duration at 3 values including the value in the #1 recipe.

4.2.1. Deposition Time

Using the standard recipe, we deposited a-Si:H for 20, 40, and 60min. The I-V corresponding curves are plotted in *Figure 30*. The I-V curve of the 20min sample bends up past 10V, which is not experienced by the 40 and 60min samples. 10V may have passed the breakdown voltage and the current may be penetrating through the ~300nm SiO_2 deposited by the standard recipe on HDPCVD as it is not a very dense SiO_2 film.

The photosensitivity ratio of all the 3 samples is at the level of 10^3 and increases slightly with the longer deposition time (*Figure 30*). The thickness of the film is proportional to the deposition time, indicating a constant deposition rate. The thicker film has a larger light absorption, inducing more carriers and resulting in more photoconductivity.

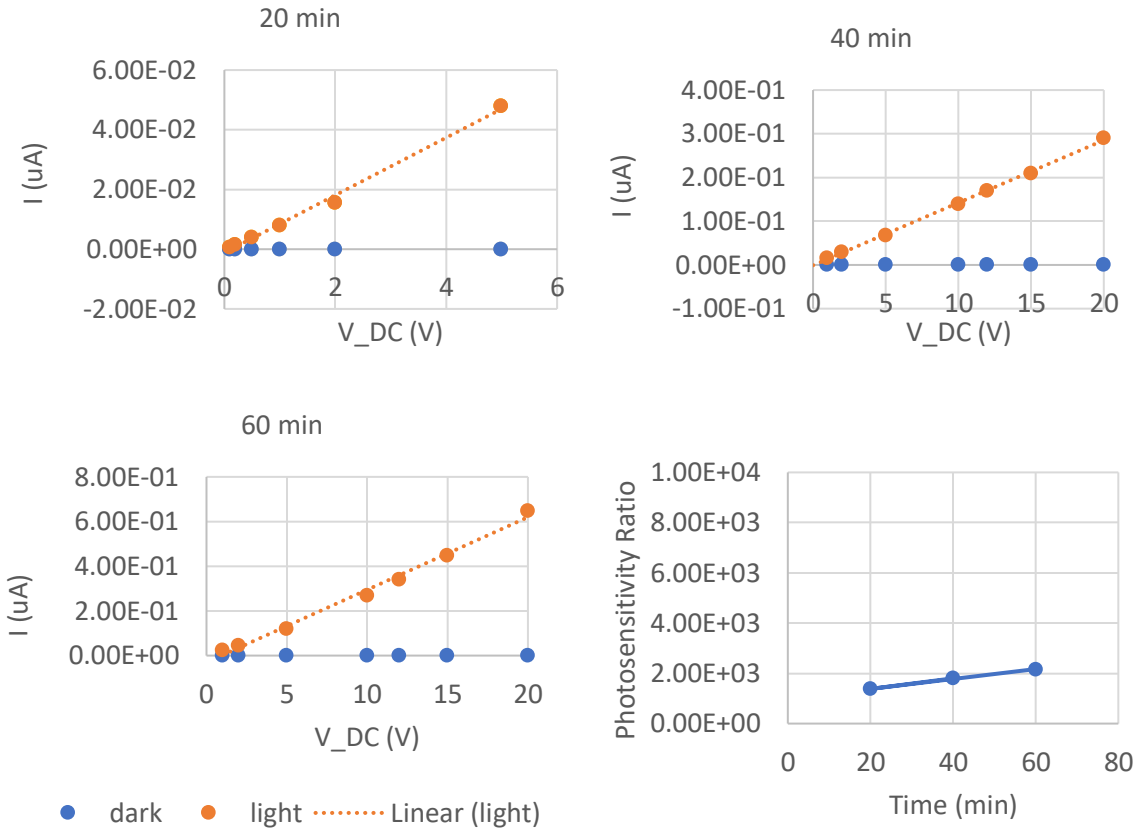

Figure 30 I-V curves of the 20, 40, and 60min samples. Photosensitivity ratio vs. deposition time duration plot.

4.2.2. Pressure

To study the deposition pressure influence on the a-Si:H photoconductivity, we varied the pressure to be 2 and 40mTorr from the standard pressure of 4mTorr. The I-V curves of the samples and the photosensitivity ratio vs. pressure plot are shown in *Figure 31*. The 40mTorr sample has a much larger dark current. At a higher pressure, the deposition rate increases, and the film may be less dense and more porous, so that the film may be less insulating. This may cause a higher dark current value to be measured. However, a higher deposition rate can result in more dangling bonds and midgap states that act as recombination centers, causing a lower photoconductivity. According to the measurement of the three samples deposited at different pressure values, we can see the photoconductivity decreases with the increasing pressure.

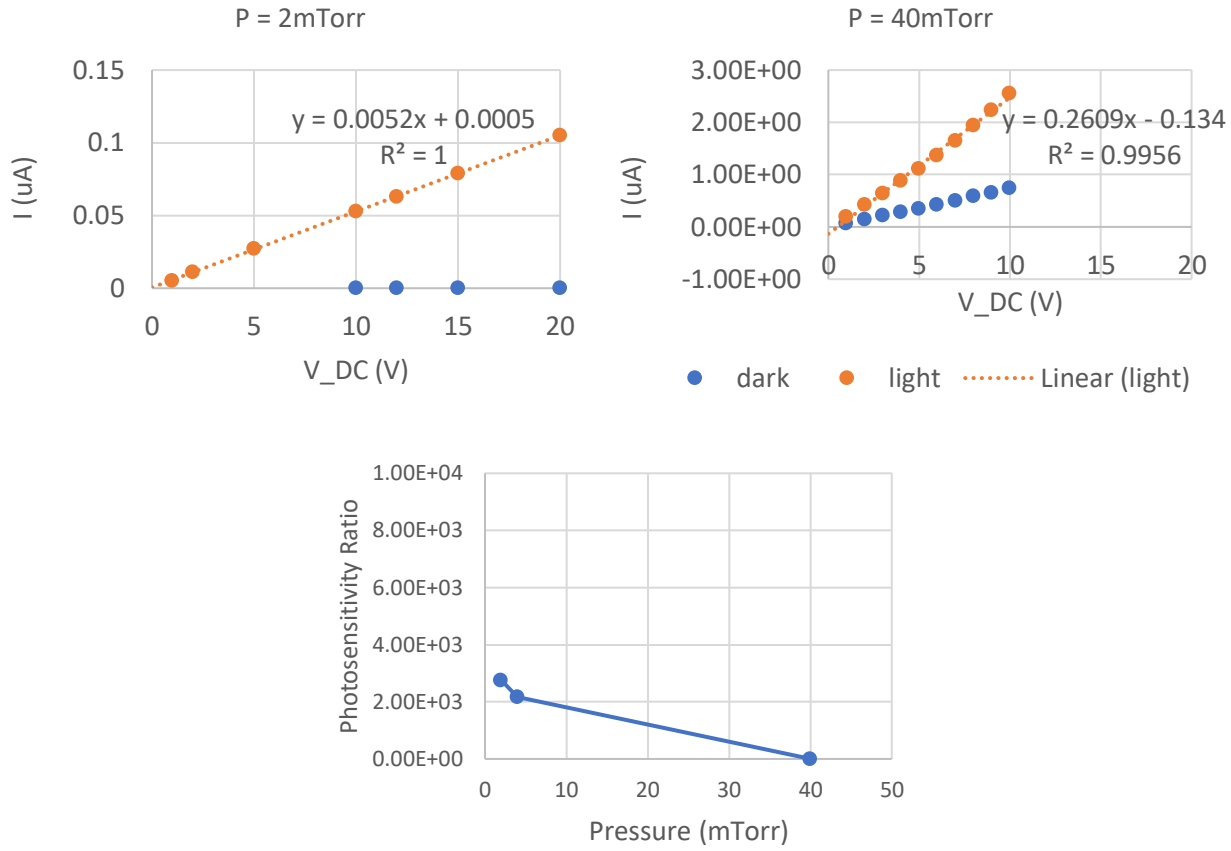

Figure 31 I-V curves of the 2 and 40mTorr samples. Photosensitivity ratio vs. pressure plot.

4.2.3. Temperature

HDPCVD utilizes inductively coupled plasma (ICP) to create a high-density plasma in the reacting chamber, which allows high quality film deposition at a much lower temperature than that is required by plasma-enhanced chemical vapor deposition (PECVD) and low-pressure chemical vapor deposition (LPCVD). The temperature of the standard recipe on HDPCVD was set to be 90°C while the lower and upper limits of the machine was 50°C and 140°C. The I-V curves of the 50°C and 140°C samples and the photosensitivity ratio vs. temperature plot are shown in *Figure 32*. The dangling bonds can be reduced by lower deposition rate and higher temperature. In principle, photoconductivity performance should be improved by increasing the temperature. However, higher temperature usually means higher deposition rate, and the photosensitivity ratio peaks at 90°C. We can observe an increase in the light current with the deposition temperature, indicating more light induced carriers. However, the dark current also increases with the deposition temperature. When the dark current was measured, there was still minimal ambient light that might have induced some current, contributing to a higher measured dark current value. As a result, the measured photosensitivity ratio does not monotonically increase with the temperature. There may be a tradeoff between higher temperature and lower deposition rate. At 140°C, the other parameters in the recipe could be tuned to lower the deposition rate, which may lead to better photoconductivity.

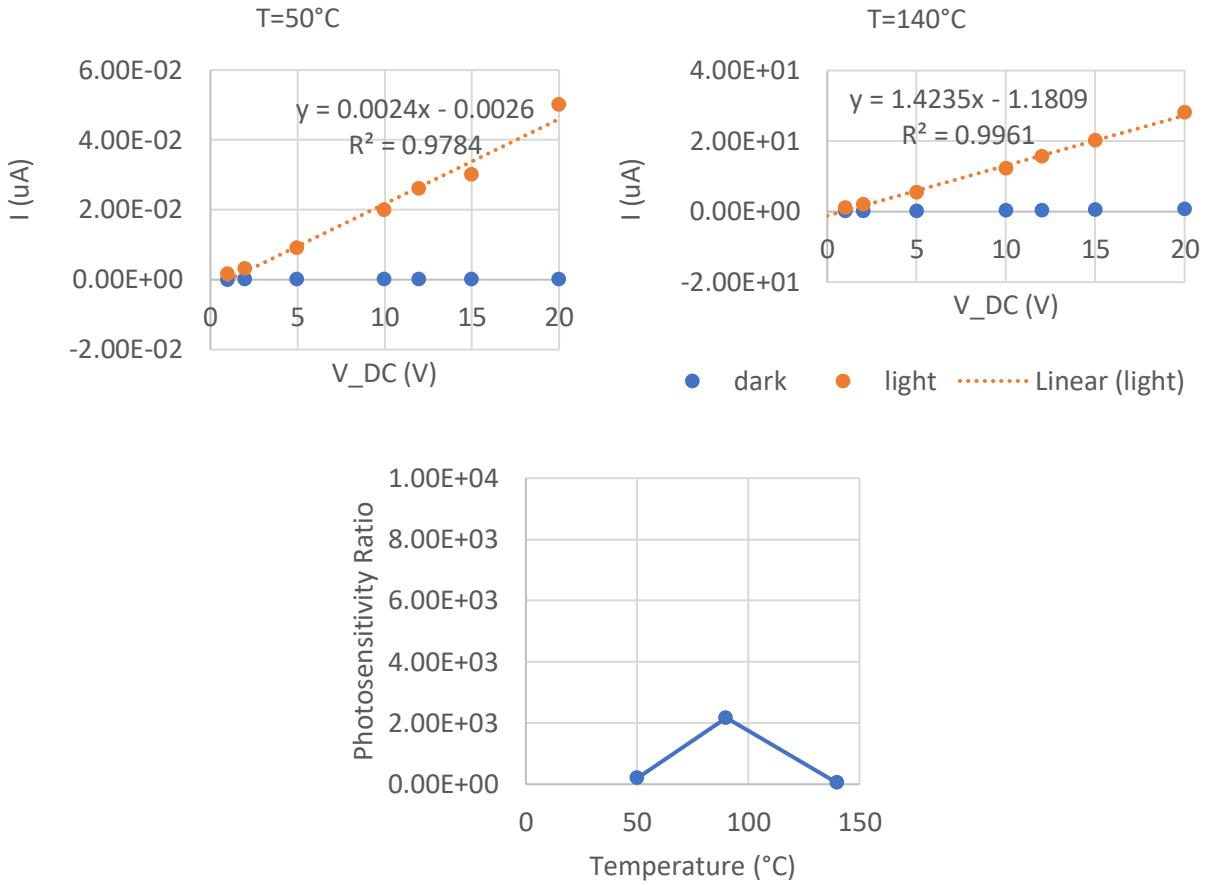

Figure 32 I-V curves of 50°C and 140°C samples. Photosensitivity ratio vs. temperature plot.

4.2.4. Bias Power

The higher the bias power, the lower the deposition rate, and a non-zero bias power can flip the process from deposition to etching. The standard recipe has a 0W bias power. We deposited additional samples at 25, 50 and 100W. The 100W sample has the SiO_2 completely etched, and part of the Si substrate etched. The I-V curves of the 25 and 50W samples and the photosensitivity ratio vs. bias power plot are shown in *Figure 33*. The 50W sample shows a Schottky contact instead of ohmic. Its surface shows some concentric rainbow pattern. The a-Si:H film may be very thin so that with a higher supplied voltage the current could penetrate through the SiO_2 layer and travel through the Si substrate. In addition, the contact type between Ti and a-Si could be altered by a-Si:H film surface character. The 50W bias power may have contributed to a significant enough surface quality alteration causing the change of contact type.

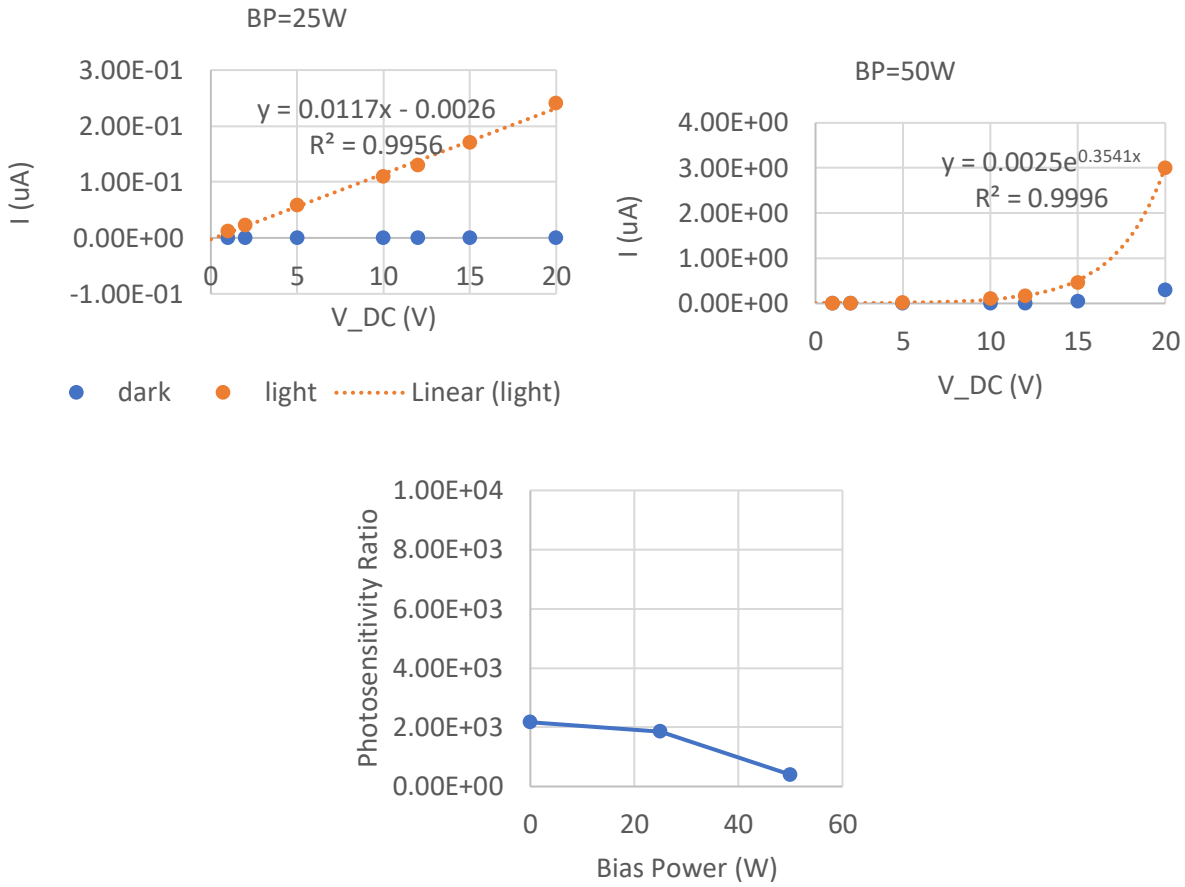

Figure 33 I-V curves of 25 and 50W samples. Photosensitivity ratio vs. bias power plot.

4.2.5. Argon (Ar) Flow Rate

Keeping every other parameter in the standard recipe the same, we tuned the Ar flow rate to be 5 and 100sccm, while that of the standard recipe is 40sccm. The I-V curves of the 5 and 100sccm Ar flow rate samples and the photosensitivity ratio vs. Ar flow rate plot are shown in *Figure 34*. When the chamber pressure is maintained, increasing only the Ar flow rate results in a lower concentration of the SiH_4 gas flow. As SiH_4 is the reactant that forms the a-Si film, a lower SiH_4 concentration corresponds to a lower deposition rate. The photosensitivity increases monotonically with the Ar flow rate and the increase seems to be saturating as Ar flow rate approaches 100sccm. This may be because the dynamic equilibrium between Ar and SiH_4 flow reaches at a certain point to maintain the constant chamber pressure.

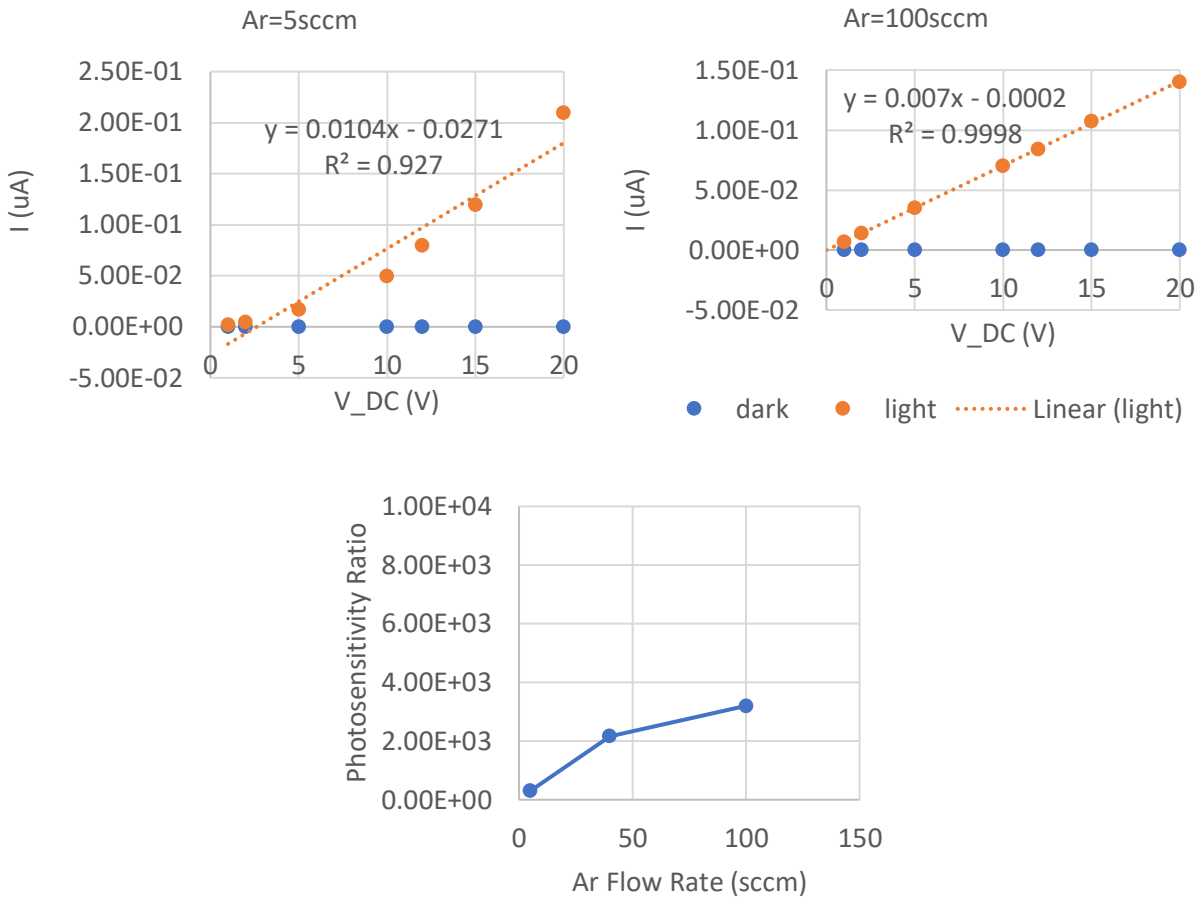

Figure 34 I-V curves of 5 and 100sccm Ar flow rate samples. Photosensitivity ratio vs. Ar flow rate plot

4.2.6. Silane (SiH_4) Flow Rate

The I-V curves of the 15 and 35sccm SiH_4 flow rate samples and the photosensitivity ratio vs. SiH_4 flow rate plot are shown in *Figure 35*. The deposition rate increases with the reactant gas flow. As a result, more dangling bonds may be created during the deposition. On the other hand, a thicker film could have higher light absorption. The effects of the film thickness and the film quality may have contributed to the quadratic relationship between the photoconductivity and the SiH_4 flow rate. However, the very low photoconductivity at 15sccm is still surprising. Since we did not repeat the measurements, it is possible that this data point is an outlier.

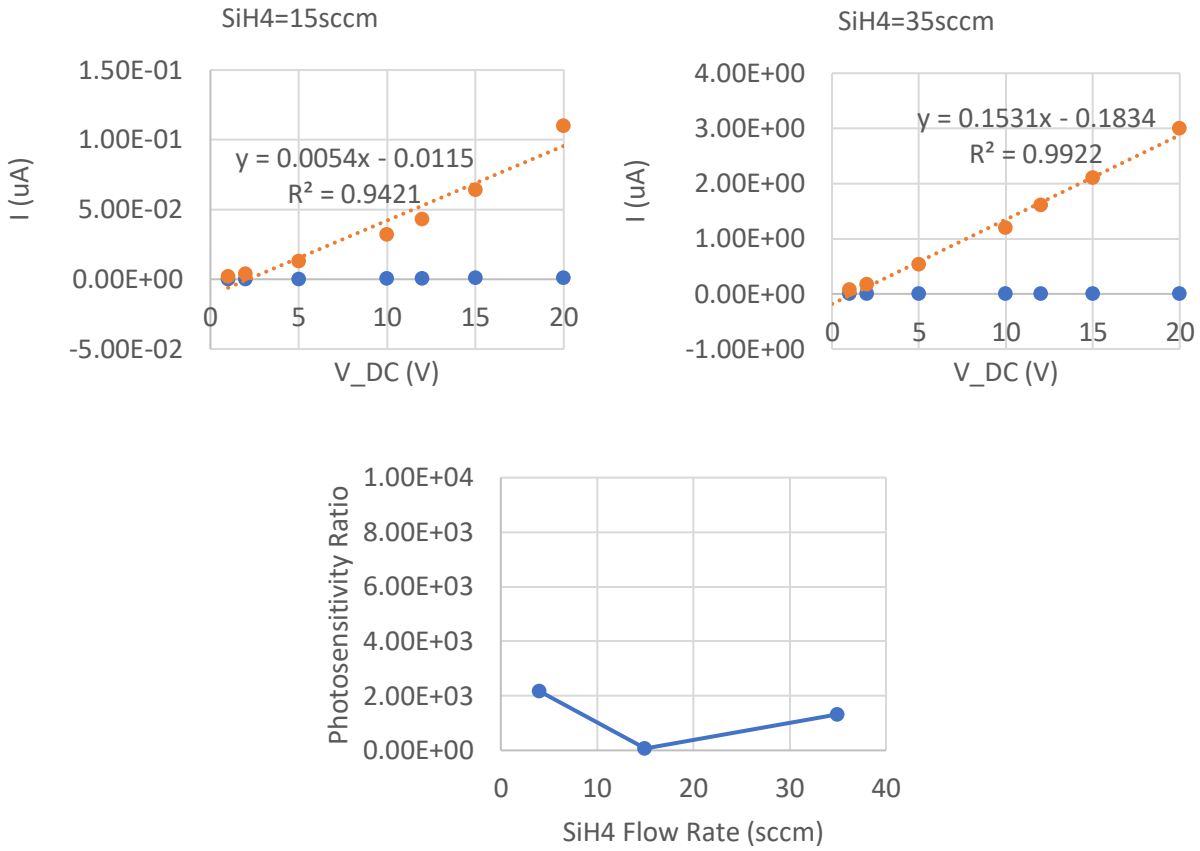

Figure 35. I-V curves of 15 and 35sccm SiH_4 flow rate samples. Photosensitivity ratio vs. SiH_4 flow rate plot

4.2.7. Inductively Coupled Plasma (ICP) Power

HDPCVD utilizes inductively coupled plasma (ICP) to create a high-density plasma in the reacting chamber, which allows high quality film deposition at a much lower temperature than that is required by PECVD and LPCVD. The I-V curves of the 300, 1800, and 2000W samples and the photosensitivity ratio vs. ICP power plot are shown in *Figure 36*. The sample deposited at 1800W ICP power had the best photoconductive performance. The I-V measurement for this sample was repeated for three times. Error bars are shown in the corresponding ICP=1800W I-V curve in *Figure 36.*

4.2.8. Interaction Effects of ICP Power and SiH_4 Flow Rate

To study the interaction effect of the two main effects, i.e., ICP power and SiH_4 flow rate, we chose two values for each parameter and ran all 4 combinations of them. For ICP power, the values are 1800 and 2000W. For SiH_4 flow rate, the values are 4 and 35sccm. I-V curves of ICP=1800W, SiH_4 = 35sccm and ICP=2000W, SiH_4 = 35sccm samples and photosensitivity ratio and film thickness vs. ICP power plot are shown in *Figure 37*. Theoretically [13], the lower the density of dangling bonds, the higher the photoconductivity. The dangling bonds can be reduced by lower deposition rate and higher temperature. The midgap states given by the dangling bonds act as recombination centers and are detrimental to photoconductivity performance. At silane rate of 35sccm, with increasing ICP power, the deposition rate increases and the photoconductivity decreases, which agrees well with the theory. However, at silane rate of 4sccm, the photoconductivity spikes at ICP = 1800W, which interestingly

corresponds to the thickest film/highest deposition rate, which follows a different trend from that of the 35sccm silane flow rate. This indicates an interaction effect between silane flow rate and ICP on the photoconductivity. The theory and principle behind these phenomena would be interesting to study further.

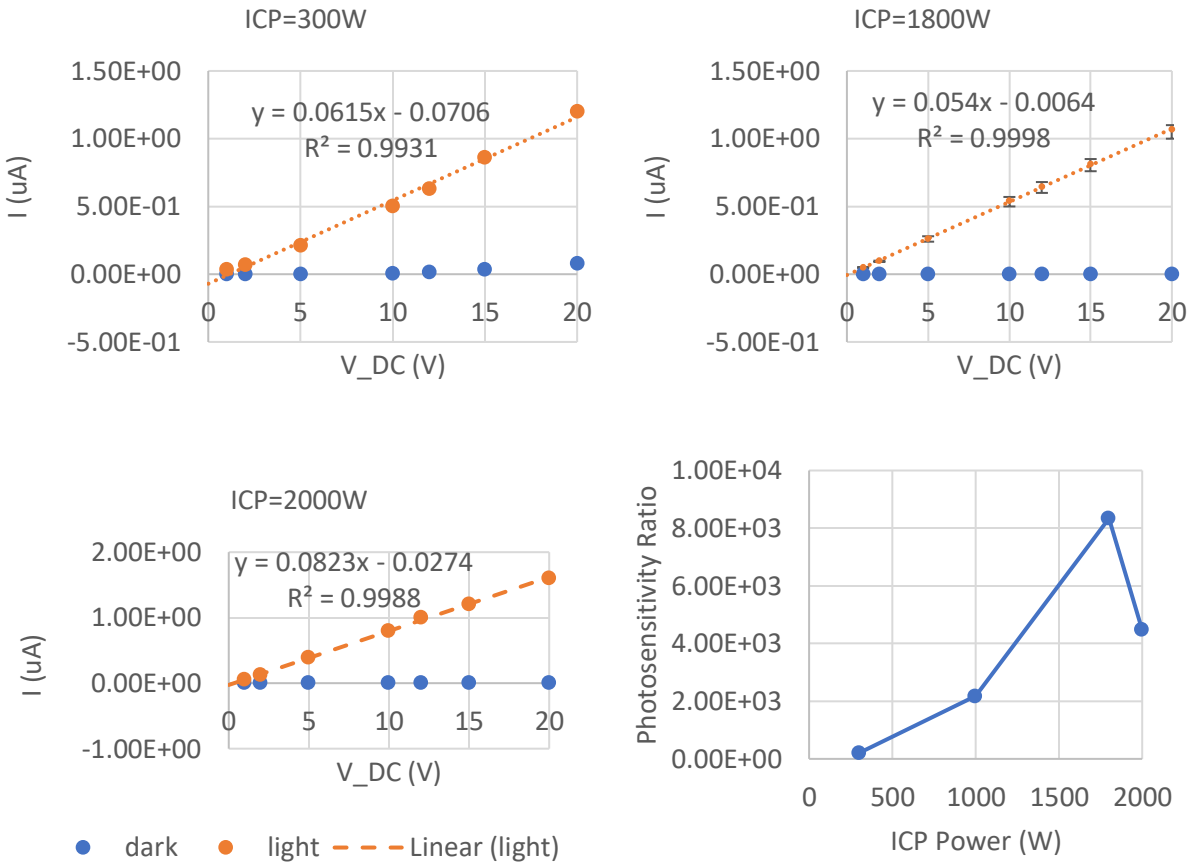

Figure 36. IV curves of 300, 1800, and 2000W ICP power samples. Photosensitivity ratio vs. ICP power plot

Most of the current measurements has a settling time, so the readings were determined manually, which may have contributed to some errors in the photosensitivity ratio measurement.

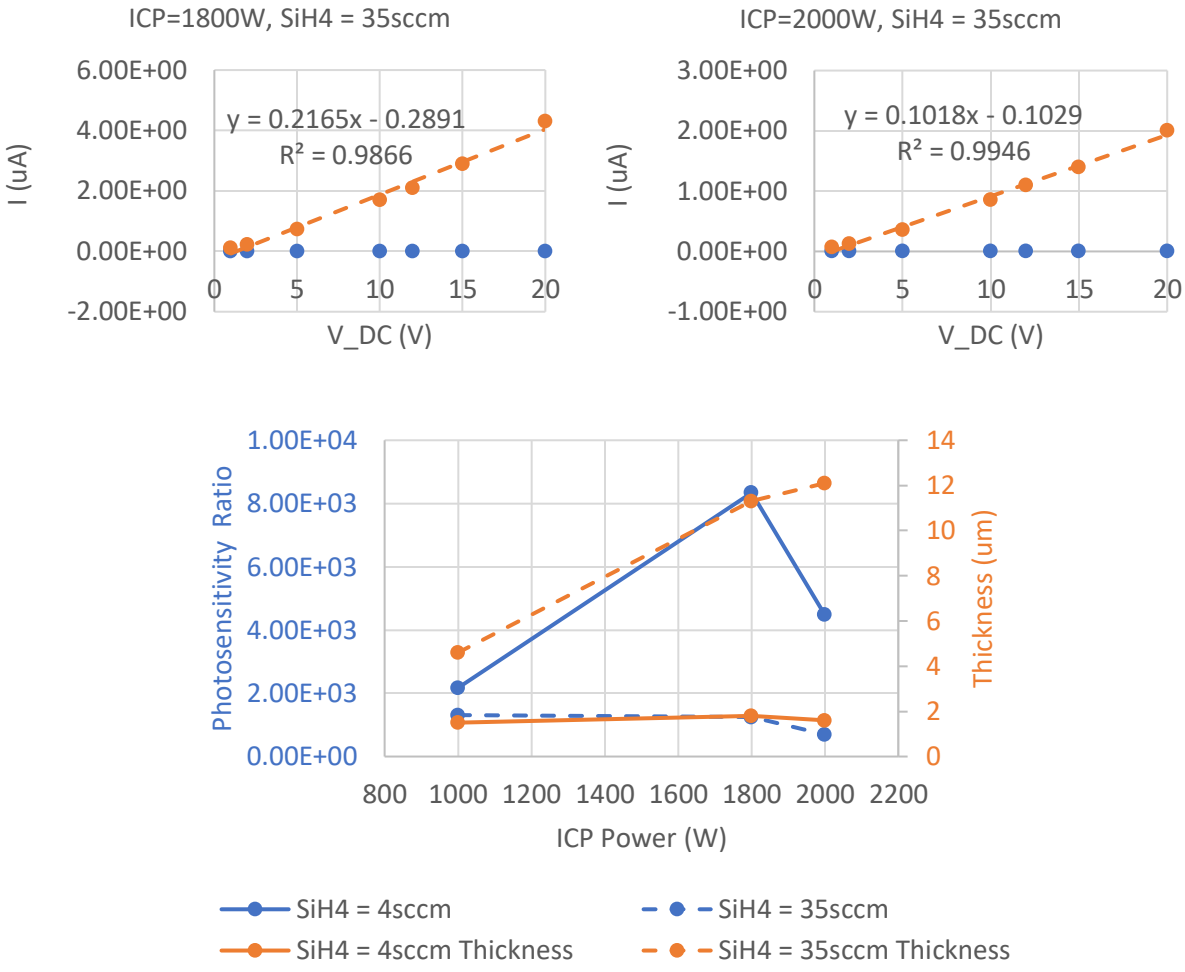

Figure 37 IV curves of ICP=1800W, SiH4 = 35sccm and ICP=2000W, SiH4 = 35sccm samples. Photosensitivity ratio and film thickness vs. ICP power plot

5. Conclusions

In conclusion, we have found a recipe that increases the photoconductivity almost *four-fold* from the standard recipe (*Table 7*). The most interesting data we collected are summarized in *Table 8*.

Table 7 Summary of the a-Si:H recipe for maximal photoconductivity.

Optimal Photoconductivity Recipe	
Tool	HDPCVD
Pressure	4mTorr
Temperature	90°C
ICP Power	1800W
Bias Power	0W
Ar Flow Rate	40sccm
SiH4 Flow Rate	4sccm

Table 8 Summary of thickness, surface roughness, and uniformity measurements of selected samples.

Recipe Name	ICP Power (W)	SiH_4 Flow Rate(sccm)	Photosensitivity Ratio	Thickness (um)	Surface Roughness Sq (nm)	Surface Roughness Sa (nm)	Uniformity (%)
#1	1000	4	2.17E+03	1.5	21.90	17.92	1.99
#15	1000	35	1.31E+03	4.6	7.28	5.81	N/A
#9	1800	4	8.34E+03	1.8	6.72	4.577	0.98
#2-1	1800	35	1.25E+03	11.3	14.53	11.75	0.14
#2-2	2000	4	4.48E+03	1.6	0.58	0.45	0.27
#2-3	2000	35	6.97E+02	12.1	19.83	16.17	N/A

6. Future Work

Beyond the scope of this class, there are several things we consider worthwhile trying. First, fine-tuning on ICP power along with the other parameters such as temperature, Ar flow rate, Ar/SiH_4 ratio seems promising for a higher photoconductivity a-Si:H recipe. Since unpassivated dangling bonds in a-Si:H film are detrimental to its photoconductivity performance and they can be reduced by higher temperature and lower deposition rate, a better parameter combination for a higher temperature recipe could be promising. Because ccp-dep (PECVD) deposits at a much higher temperature of 350°C, a comparison between the a-Si:H films deposited by ccp-dep and HDPCVD would be interesting. In addition, density and stress are important characteristics of thin film deposition. Measurements of these quantities would be useful to provide additional information and insights for the photoconductivity behavior of different a-Si:H films. The density can be studied by etching. A lower etching rate indicates a denser film. Finally, to develop an a-Si:H recipe of higher photoconductivity in a more systematic way, a study of the theory and principle behind the data and phenomena would be essential. The microstructure of the film plays an important role in light-induced charge carrier. Dangling bonds behaving as recombination centers are detrimental to photoconductivity performance. The microvoid density can be evaluated from Fourier transform infrared thermography (FTIR). Hydrogen dilution during deposition and annealing after deposition are approaches to reduce the dangling bond density and thus improve the photoconductivity [13]. The HDPCVD tool at SNF does not have a H_2 gas line, so hydrogen dilution method may only be explored on other tools.

7. Acknowledgement

Huge thanks to Usha Raghuram, Swaroop Kommera, Lavendra Yadav Mandyam, Tom Carver, Ludwig Galambor, Yao-Te Cheng, Mohammad Asif Zaman, Prof. Bert Hesselink, and Prof. Roger Howe for their guidance and many helpful suggestions and insights throughout the quarter!

Special thanks to Prof. Boris Murmann for the sourcemeter!

Reference

1. Dincer, I. (2018). Comprehensive energy systems. Elsevier.
2. Brinza, M., Willekens, J., Benkhedir, M. L., Emelianova, E. V., & Adriaenssens, G. J. (2005). Photoconductivity methods in materials research. Journal of Materials Science: Materials in Electronics, 16(11), 703-713.
3. Vaněček, M., Kočka, J., Poruba, A., & Fejfar, A. (1995). Direct measurement of the deep defect density in thin amorphous silicon films with the ‘‘absolute’’ constant photocurrent method. Journal of applied physics, 78(10), 6203-6210.
4. Malik, H. K., Juneja, S., & Kumar, S. (2019). Employing constant photocurrent method for the study of defects in silicon thin films. Journal of Theoretical and Applied Physics, 13(2), 107-113.
5. Abel, C. D., & Bauer, G. H. (1993). Evaluation of the steady-state photocarrier grating technique with respect to A-Si: H and its application to A-Si1–X GeX: H alloys. Progress in Photovoltaics: Research and Applications, 1(4), 269-278.
6. Srivastava, A., Agarwal, P., & Agarwal, S. C. (2002). Origin of lateral photovoltage in hydrogenated amorphous silicon and silicon germanium thin films. Journal of non-crystalline solids, 299, 430-433.
7. Longeaud, C., Ventosinos, F., & Schmidt, J. A. (2012). Determination of hydrogenated amorphous silicon electronic transport parameters and density of states using several photoconductivity techniques. Journal of Applied Physics, 112(2), 023709.
8. Oheda, H. (1981). Phase-shift analysis of modulated photocurrent: Its application to the determination of the energetic distribution of gap states. Journal Of Applied Physics, 52(11), 6693-6700.
9. Chiou, P. Y., Ohta, A. T., & Wu, M. C. (2005). Massively parallel manipulation of single cells and microparticles using optical images. Nature, 436(7049), 370-372.
10. Safa Kasap, Peter Capper (2017). Springer Handbook of Electronic and Photonic Materials
11. Kanicki, J., & Bullock, D. (1986). Ohmic and Quasi-Ohmic Contacts to Hydrogenated Amorphous Silicon Thin Films. MRS Proceedings, 70, 379. doi:10.1557/PROC-70-379
12. R.A. Street (1991). Hydrogenated Amorphous Silicon, Cambridge University Press.
13. Arvind Shah (2010). Thin-Film Silicon Solar Cells, EPFL Press. doi: 10.1016/B978-0-12-809921-6.00008-2
14. Wu, M. C. (2011). Optoelectronic tweezers. Nature Photonics, 5(6), 322-324.
15. Zaman, M. A., Padhy, P., Cheng, Y. T., Galambos, L., & Hesselink, L. (2020). Optoelectronic tweezers with a non-uniform background field. Applied Physics Letters, 117(17), 171102.

Appendix

Light Source Intensity Measurement

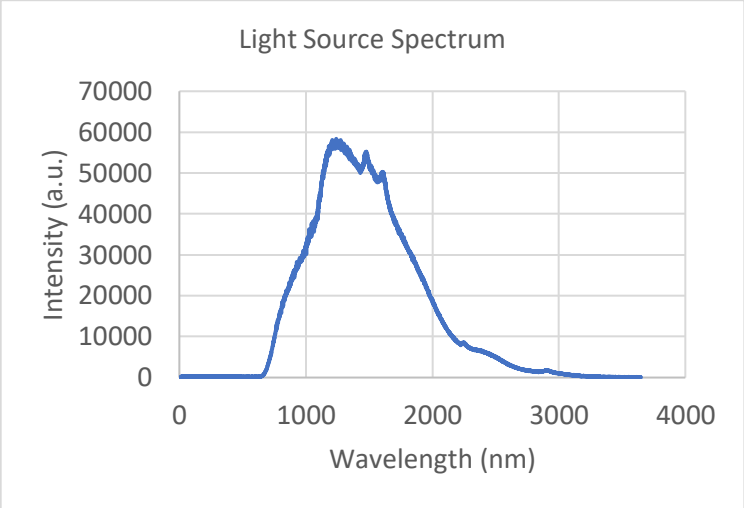

Figure A1 Spectrum of the light source used in the photoconductivity measurement setup

To estimate the light source intensity, we used a photodiode (model: UDT PIN-25D 0010-1). The photodiode was placed at the sample holder. The relative data was recorded in *Table A1*.

Table A1 Light source intensity

Parameter	White light	Green light
Responsivity (A/W)	0.5	0.3
Current (mA)	12	0.7
Power (mW)	24	2.3
Irradiance (mW/cm^2)	96	9.3
*Light spot area = 0.25cm^2		
*Photodiode model = UDT PIN-25D 0010-1		

Substrate Comparison

At the beginning of this project, we have tested 3 substrates for the a-Si deposition. First is the ITO coated glass slide with silver busbar, which can be purchased from a vendor and thus saves us from depositing contact pads defined by lithography. This arrangement also has the advantage of the bottom illumination potential. The contacts with the a-Si:H film are made by the bottom ITO layer and a conductive tape placed on the top. We tried both copper and aluminum tapes but struggled with making stable ohmic contact. Then we tried glass and silicon wafers. Glass wafer has the advantage of bottom illumination possibility and does not require an additional SiO_2 deposition that is required by the Si wafer. Unfortunately, because of the supply chain issue, we had to settle for the Si wafers. *Figure A2* shows the photoconductivity measurement arrangements of samples with ITO coated glass slide and Si substrates. *Figure A3* shows the I-V curves of two samples, the 60min standard recipe on glass wafer and the 20min standard recipe on Si wafer. To image the sample with glass substrate under SEM, a 10nm Pd/Au layer is sputtered by Cressington Sputter Coater. *Figure A4* is the SEM image of the glass substrate sample. Both samples have the same Au/Ti contact pads. When the applied voltage is less than 10V, the glass sample has a larger light current than the Si sample, which is expected because the

glass sample has a thicker film. However, the I-V curve of the Si sample bends up past 10V. This may be because the Si sample has a thinner a-Si film and the current penetrates through the SiO_2 layer to the Si substrate, resulting in the current to hype. We have also determined the deposition rates on glass and silicon substrates are similar. For the future study, glass wafer is the preferred substrate. A denser and higher quality SiO_2 layer could be deposited on Si substrate by LPCVD or a different recipe on HDPCVD if glass wafer is not a realistic option.

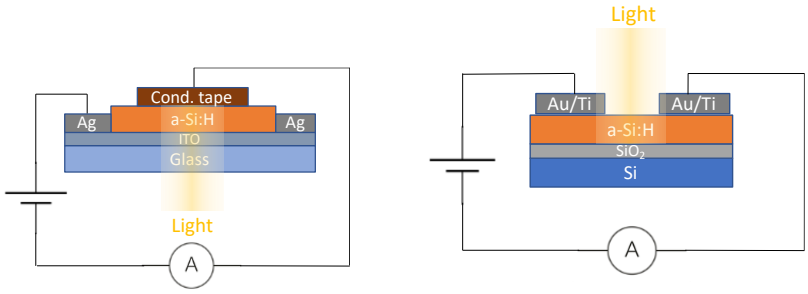

Figure A2. Photoconductivity measurement arrangements of samples with ITO coated glass slide and Si substrates.

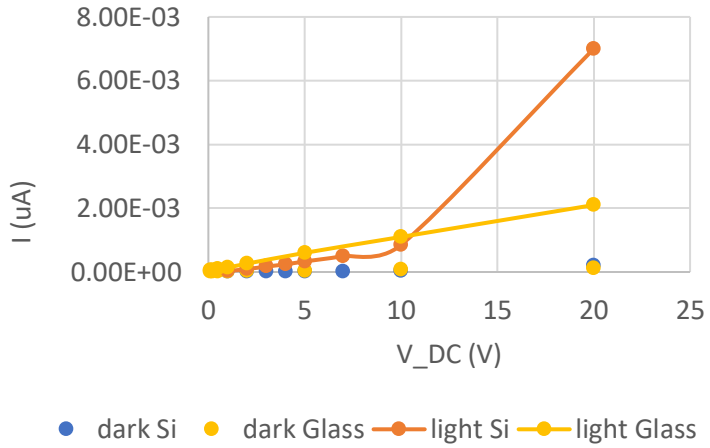

Figure A3 I-V curves of the 60min on glass sample and the 20min on Si sample (both deposited with #1 standard recipe).

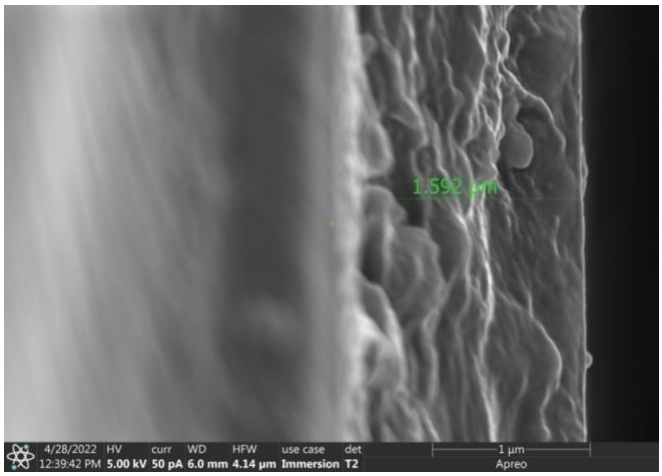

Figure A4 Cross section SEM image of the 60min on glass substrate sample

Woollam Thickness Verification for SiO_2

Woollam thickness verification for Figure 10 (SiO_2 deposited on Si substrate) is shown in *Figure A5*. Both the first and the last samples among a batch of nine SiO_2 coated Si wafers are measured to have a thickness of approximately 340nm.

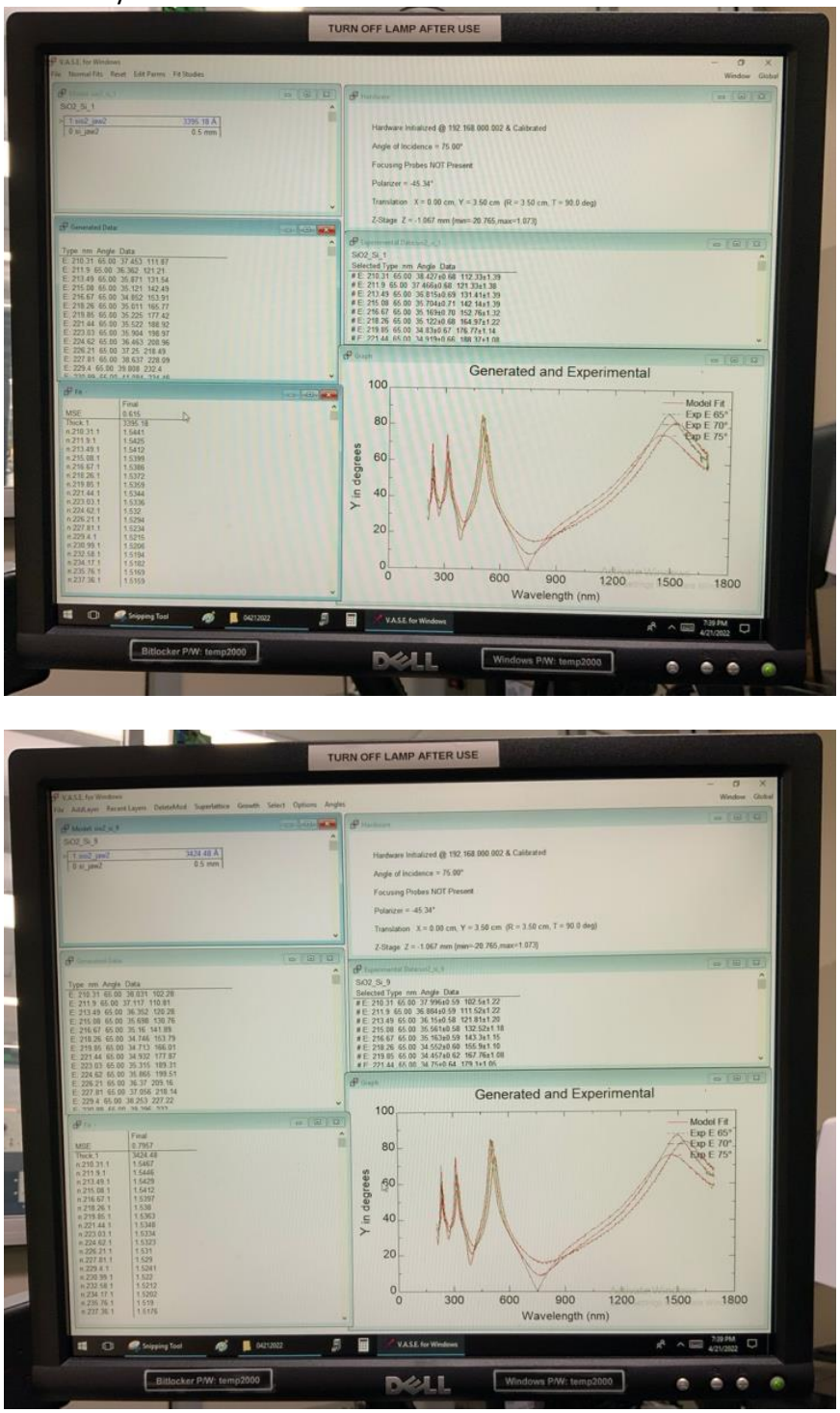

Figure A5 Woollam thickness verification for the first (top) and the last (bottom) samples among a batch of nine samples.

Woollam Fitting of a-Si:H Thickness with Different Initial Values

Figure A6 shows the a-Si:H thickness fitting for #1 standard recipe with different initial values. An initial guessing thickness of both 1μm and 1.4μm gives similar good fitting which indicates the fact that a relative accurate thickness guessing is required to obtain a good estimate of thin film thickness.

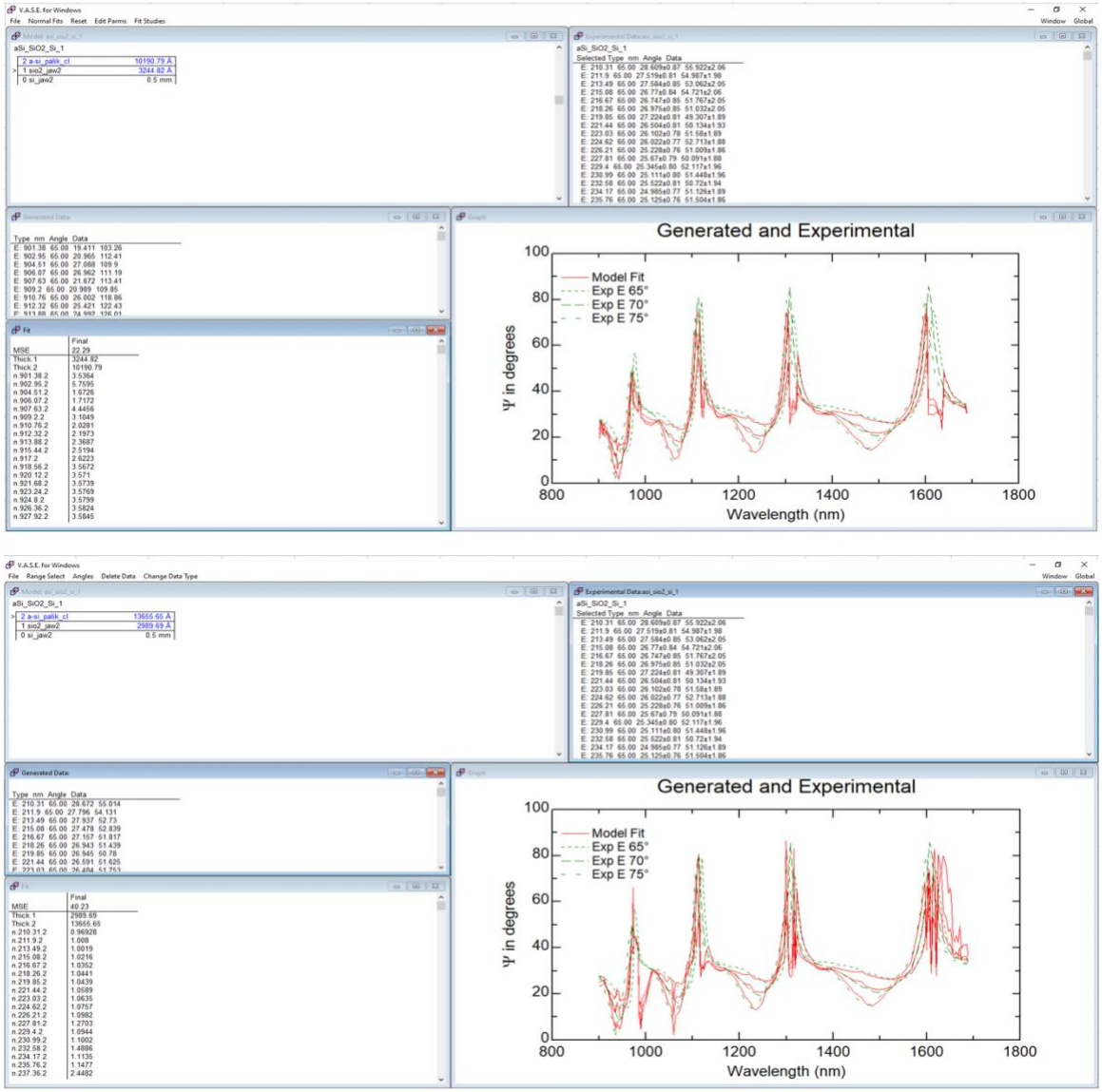

Figure A6 Woollam fitting of a-Si:H thickness for #1 standard recipe with initial value 1μm (top) and 1.4μm (bottom).

Figure A7 shows the full spectrum measured data from ellipsometry and the corresponding Woollam fitting. There are violent fluctuations for the wavelength range from 600nm to 900nm. It makes the model struggle to obtain a precise fitting within this range. Restricted by the time, we intercept and only fit for the wavelength range from 900nm to 1700nm where severe oscillations are avoided while enough features are included for a reasonable fitting. In the subsequent study, we would try to use the refractive indices data of intermediate SiO_2 layer from ellipsometry for the fitting. It might provide better fitting precision even for the full spectrum.

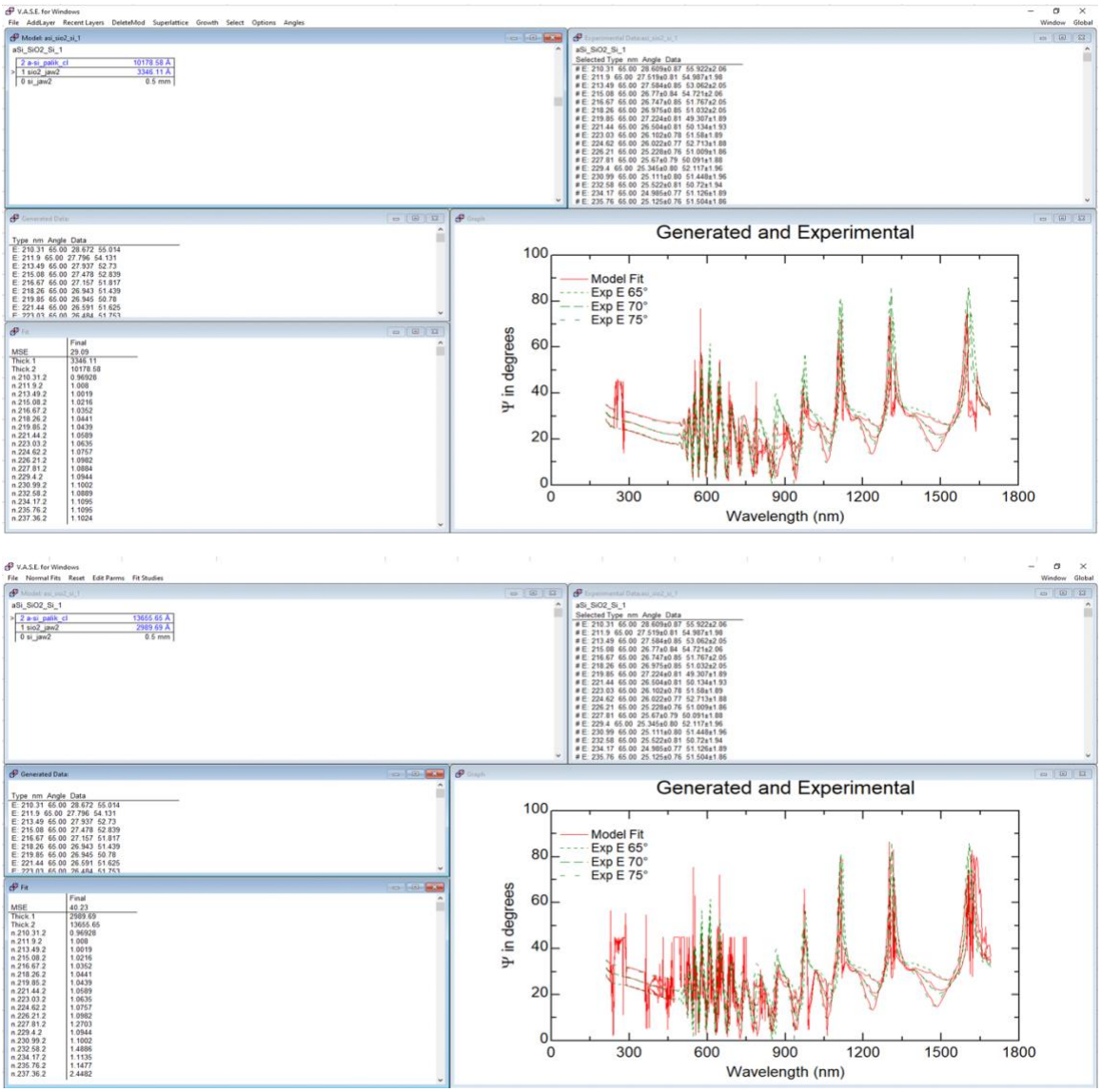

Figure A7 Full-spectrum Woollam fitting of a-Si:H thickness for #1 standard recipe with initial value 1μm (top) and 1.4μm (bottom).